A new method for the quantification of ambient particulate matter emission fluxes

Stergios Vratolis[1], Evangelia Diapouli[1], Manousos I. Manousakas[2], Susana Marta Almeida[3], Ivan Beslic[4], Zsofia Kertesz[5], Lucyna Samek[6], and Konstantinos Eleftheriadis[1]

[1]ENvironmental Radioactivity & Aerosol Technology for atmospheric & Climate ImpacT Lab, INRASTES, NCSR Demokritos, 15310 Ag. Paraskevi, Attiki, Greece
[2]Laboratory of Atmospheric Chemistry, Paul Scherrer Institute, Villigen-PSI, 5232, Switzerland
[3]Department of Nuclear Sciences and Engineering & C2TN, Instituto Superior Técnico, Universidade de Lisboa, Bobadela, Portugal
[4]Environmental Hygiene Unit, Institute for Medical Research and Occupational Health, Zagreb, 10000, Croatia
[5]Institute for Nuclear Research (ATOMKI), Bem tér 18/C, Debrecen, 4026, Hungary
[6]AGH University of Science and Technology, Faculty of Physics and Applied Computer Science, ul. Mickiewicza 30, 30-059, Krakow, Poland

Correspondence: S. Vratolis (vratolis@ipta.demokritos.gr)

Abstract. An inversion method has been developed in order to quantify the emission fluxes of certain aerosol pollution sources across a wide region in the Northern hemisphere, mainly in Europe and Western Asia. The data employed are the aerosol contribution factors deducted by Positive Matrix Factorization (PMF) on a $PM_{2.5}$ chemical composition dataset from 16 European and Asian cities for the period 2014 to 2016. The spatial resolution of the method corresponds to the geographic grid cell size of the Lagrangian particle dispersion model (FLEXPART, 1° x 1°) which was utilized for the air mass backward simulations. The area covered is also related to the location of the 16 cities under study. Species with an aerodynamic geometric mean diameter of 400 nm and 3.1 μm and geometric standard deviation of 1.6 and 2.25 respectively were used to model the ~~Secondary Sulfate and Dust~~ secondary sulfate and dust aerosol transport. PSCF analysis and Generalized Tikhonov regularization were applied so as to acquire potential source areas and quantify their emission fluxes. A significant source area for ~~Secondary Sulfate~~ secondary sulfate on the East of the Caspian Sea is indicated, when data from all stations are used. The maximum emission flux in that area is as high as 10×10^{-12} $kg * m^{-2} * s^{-1}$. When Vilnius, Dushanbe and Kurchatov data were excluded, the areas with the highest emission fluxes were the Western and Central Balkans and South Poland. The results display many similarities to the SO_2 emission maps provided by OMI-HTAP and ECLIPSE databases. For ~~Dust~~ dust aerosol, measurements from Athens, Belgrade, Debrecen, Lisbon, Tirana, and Zagreb are utilized. The west Sahara region is indicated as the most important source area and its contribution is quantified, with a maximum of 17.6×10^{-12} $kg * m^{-2} * s^{-1}$. When we apply the emission fluxes from every geographic grid cell (1° x 1°) for ~~Secondary Sulfate~~ secondary sulfate aerosol deducted with the new method to air masses originating from Vilnius, a useful approximation to the measured values is achieved.

1 Introduction

20 Atmospheric aerosol particles affect air quality, human health, atmospheric visibility, and the climate (Laden et al., 2006; Lohmann and Feichter, 2005; Pope and Dockery, 2006; Ghosh et al., 2021; Burkart et al., 2022; Pandey et al., 2021; WHO, 2021). In order to identify and quantify aerosol sources and corresponding source areas, significant effort is required by the Scientific Community. When this information is acquired, measures can be applied so as to improve air quality. Source apportionment methods are widely used for air quality management, as they provide information on the relationship between

25 air pollutant sources and their concentrations. The quantification of air pollution sources, both in terms of their sectorial and spatial origins, constitutes an essential step of the air quality management process (Wesseling et al., 2019).

This work is the follow up of the article by Almeida et al. (2020). In order to find the source areas for the pollution sources in the aforementioned publication as identified by Almeida et al. (2020) we followed the Potential Source Contribution Function analysis (PSCF) (Eleftheriadis et al., 2009) and a discrete, deterministic approach (Tikhonov regularization ,(Tikhonov et al.,

30 1995)). Discrete, deterministic approaches have a long and distinguished history in geophysics. The major advantage of these methods is their computational efficiency, with costs governed by the number of discrete basis functions used. This limits the scale of the inference task to suit available resources, but imposes strong assumptions about the properties of the model sought: we assume that it can be well-represented using the chosen set of basis functions. A drawback of any deterministic approach is the presumption that there is a single "answer" that can explain observations. In many cases, this cannot be true: available data

35 plainly lack the sensitivity required to properly constrain all components within the basis function expansion. This motivates strategies that seek to identify the full range of models that might be compatible with observations (Park et al., 2018).

This study aims to introduce a two-step method for the quantitative estimation of emissions from geographic areas using in situ stations' measurement data. In the first step, the PSCF analysis for each measurement station is produced for the target species. Based on the results, we evaluate if at a measurement station the target species are mainly transported or locally

40 produced. In the second step, including only stations for which the target species are transported, we employ the Tikhonov regularization method in order to acquire emission fluxes from each geographic source area. The use of this method can reduce the uncertainty of emission fluxes, especially from those areas in which the emission inventories have high uncertainty. Numerous source apportionment studies have been conducted on at many European and Asian cities in the past, and this method can identify the source areas of transported aerosols and quantify their emissions.

45 In the present work no a priori information was used, and a smooth solution was sought. The smooth solution is justified by the fact that SO_2 emissions are gradually converted to Secondary Sulfate secondary sulfate aerosol as they travel along with the air masses (Seinfeld and Pandis, 1998). This process takes many hours, covering probably more than one geographic grid cell ($1° \times 1°$). Dust aerosol possibly originates from multiple neighboring cells (i.e. in North Africa) and therefore a smooth solution is suitable for this case too.

50 It is important to note that the emission fluxes retrieved are subject to air mass transport paths, atmospheric conditions and atmospheric chemistry. In other words, if a geographic grid cell emits a pollutant, but air mass transport does not allow these emissions to reach any of the measurement stations in the study, this cell will not be attributed the emission flux that it has.

For species like ~~Secondary Sulfate~~secondary sulfate, identical precursor gases emission fluxes could lead to different aerosol concentrations, depending on atmospheric conditions and chemistry. It is also possible that locally produced aerosol (that is within the station grid cell) ~~,~~cannot be correctly associated to residence time in the grid cell. That is because emission fluxes in the vicinity of the measurement stations have a very small residence time until they arrive to the station and a very high impact on the measured concentration. Despite these potential problems, the information on specific geographic grid cells that actually impact the measurement stations area is focused on where mitigation measures for long range transport must be applied.

From now on, we refer to "source apportioned concentration by PMF" as "concentration" and to "geographic grid cell source areas emission fluxes" as "emission fluxes". NE corresponds to North-East, NW to North-West, SE to South-East and SW to South-West.

2 Materials and Methods

2.1 PM sampling stations and filter analysis

More than 2,200 $PM_{2.5}$ samples were collected in urban and suburban background stations from 16 European and Central Asian cities (Tirana, Zagreb, Chisinau, Athens, Skopje, Debrecen, Banja-Luka, Sofia, Belgrade, Krakow, Montenegro, Kurchatov, Dushanbe, Vilnius, Lisbon, Ankara). Ankara and Belgrade stations are reported as suburban background by ~~(Almeida et al., 2020)~~ Almeida et al. (2020), while all other stations are reported as urban background. Sampling was performed mostly in 24-h periods, every third day, between January 2014 and December 2016. Particles were sampled on PTFE, polycarbonate, cellulose nitrate, cellulose and quartz filters by means of low and medium volume samplers.

Before and after sampling, filters were weighed in the laboratories located in each city by means of a microbalance using the procedure described in ~~EN12341~~EN12341 (1998). Filters were subsequently analyzed by several analytical techniques for the determination of major and trace elements, elemental and organic carbon, black carbon, and water soluble ions.

The Positive Matrix Factorization receptor model (EPA PMF 5.0, Brown et al. (2015)) was applied and sources were acquired for each city.

Due to the high number of cities involved in this work, it was not possible to fully harmonize the used methods, which introduces a level of uncertainty in the obtained results and especially in their comparison. Source apportionment of $PM_{2.5}$ was performed by receptor modeling that is based on the mass conservation principle. Further uncertainties to the source apportionment results ~~are~~ were introduced by the fact that at the stations of Chisinau, Sofia, Niksic, Lisbon, Ankara, and Vilnius only 50 filter samples are available.

We have not applied PMF to less than 50 samples in any of the cities. ~~We applied PMF analysis on datasets with 50 samples from 6 cities (Chisinau, Sofia, Vilnius, Niksic, Lisbon, and Ankara).~~ 50 samples have been recorded as the minimum necessary for a meaningful source apportionment analysis according to (Manousakas et al., 2017b; Johnson et al., 2011). Having said that, it has been identified in the past that small datasets (number of samples close to 50) pose an extra challenge when used for PMF because the solution is strongly affected by rotational ambiguity, and the overall uncertainty is increased. Before using the results, we have fully assessed the uncertainty of the SA solution using the enhanced tool offered by EPA PMF 5.0. The
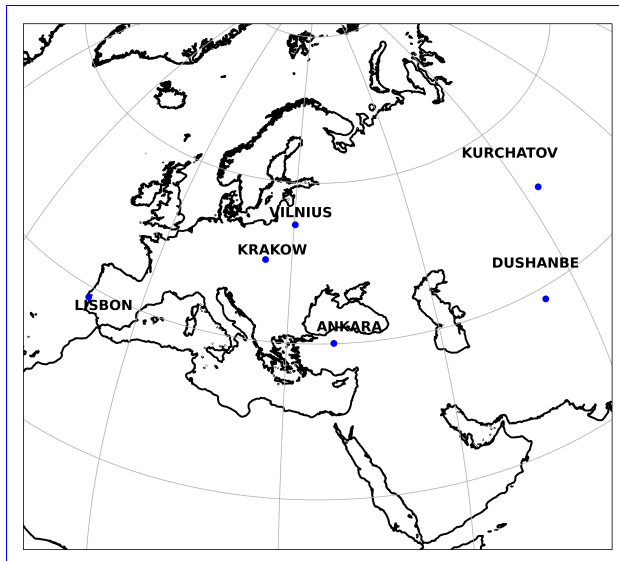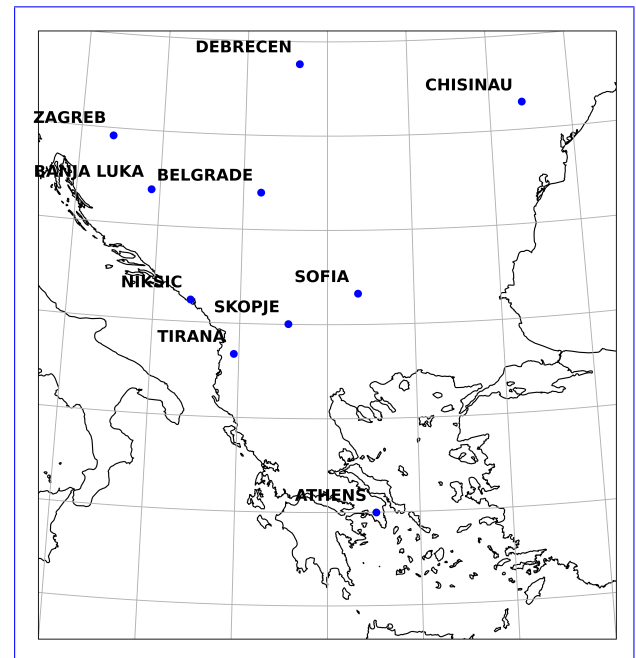
(a)   (b)

Figure 1. Urban background and suburban background measurement stations included in the study. Ankara, Dushanbe, Vilnius, Krakow, Kurchatov, and Lisbon sampling locations are depicted in subfigure (a), while Athens, Banja-Luka, Belgrade, Chisinau, Debrecen, Niksic, Skopje, Sofia, Tirana, and Zagreb sampling locations are depicted in subfigure (b).

uncertainty was within acceptable limits. We included these measurements because they are valuable, as aerosol data from these areas are scarce, and also, including them would diversify the origin of air masses used in the identification of source areas and emission fluxes, making our results more precise.

More details can be obtained in (Almeida et al., 2020), where the measurement stations, $PM_{2.5}$ analysis techniques used, 90 and PMF results are described in detail.

2.2 Flexible Particle Dispersion Model (FLEXPART)

The Flexible Particle Dispersion Model (FLEXPART) was used in order to acquire residence times over geographic grid cells (sensitivity) (Stohl et al., 2005, 2009). These residence times indicate how sensitive the measurements at a station are to emissions occurring at each geographic grid cell. FLEXPART runs account for grid scale wind as well as for turbulent 95 and mesoscale wind fluctuations. Drift correction, to prevent accumulation of the released computational particles, and density correction, to account for the decrease of air density with height, were both applied. Twenty-day backward runs with the release of 4×10^4 air parcels every 3 hours beginning from each station were produced. The residence time for each of these air parcels over each grid cell is was calculated. Then the average is was taken for all air parcels for each grid cell. This is the sensitivity

for each 3 hours. We then sum these 3-hour sensitivities so as to correspond exactly to each filter sampling time. The aerosol species carried by the air parcels were ~~Secondary Sulfate~~ secondary sulfate (400 nm aerodynamic geometric mean diameter, 1.6 standard deviation) and ~~Dust~~ dust (3.1 μm aerodynamic geometric mean diameter, 2.25 standard deviation). Wet and dry deposition of these species was also included in the ~~results~~ model. Residence times in each grid cell, for a height range from 0 to 500 m above ground level (agl), are used for this study. The height was chosen so as to include sources within the boundary layer for all geographic grid cells. Chemical reactions were not simulated in the backward runs.

The properties of the species were chosen based on the work published by (Gini et al., 2022), where an 11-stage low pressure Berner impactor was used. The Berner impactor cut sizes range from 0.03 μm to 13.35 μm at a flow rate of 26 $l*min^{-1}$. Gini et al. (2022) determined the elemental composition of the collected samples by energy dispersive X-ray fluorescence spectroscopy (XRF).

In the case of ~~Secondary Sulfate~~ secondary sulfate, it is important to keep in mind that SO_2 is the primary emitted species and ~~Secondary Sulfate~~ secondary sulfate is produced in the atmosphere through chemical reactions in gas and liquid phase. In order to calculate the uncertainty that this error induces to the calculated footprint, we refer to residence times in the atmosphere reported by (Seinfeld and Pandis, 1998), page 66. The SO_2 mean residence time reported due to dry deposition is 60 hours, its residence time due to wet deposition is 100 hours, and its residence time due to transformation to ~~Secondary Sulfate~~ secondary sulfate is 80 hours. The resulting SO_2 residence time due to wet and dry deposition is 37.5 hours, while if we also include the transformation to Sulfate the overall mean residence time is 25 hours. The corresponding wet and dry deposition residence time indicated for ~~Secondary Sulfate~~ secondary sulfate is 80 hours. Therefore, in such a case, SO_2 deposits (wet and dry deposition) twice as fast as ~~Secondary Sulfate~~ secondary sulfate. These calculations correspond to the mid-latitudes (45°-65° North) according to (Rodhe, 1978). FLEXPART model is provided with a ~~Secondary Sulfate~~ secondary sulfate aerosol particle size distribution and it compensates for wet and dry deposition as it follows the species backward in time. The error in the calculation of the residence time in each geographic grid cell is mainly due to not accounting for the enhanced deposition of SO_2 for 1-2 days just after emission. But this enhanced wet and dry deposition for SO_2 should be applied only for a small fraction of the travel time. The mean error in residence time due to this discrepancy is expected to be close to 10%.

It should be noted that we do not present emission fluxes of SO_2, but the origin of ~~Secondary Sulfate~~ secondary sulfate aerosol measured at each station, if it was produced as such in the emitting grid cell. Therefore we report the combined effect of SO_2 emissions, air mass transport and environmental conditions that produce the ~~Secondary Sulfate~~ secondary sulfate aerosol measured in the stations participating in the study. That is why ~~the authors~~ we believe that the fluxes derived cannot be applied to very distant measurement stations, whose environmental conditions might be very different from the stations in the study. Also, the estimated error ~~is~~ was calculated based on values derived for the mid-latitudes.

Since ~~Secondary Sulfate~~ secondary sulfate has a mean residence time of 80 hours in the atmosphere, as reported by (Seinfeld and Pandis, 1998), we expect that most of the ~~Secondary Sulfate~~ secondary sulfate aerosol measured at each station ~~,~~ has been produced in the atmosphere within the previous week. This would probably correspond to regional transport, not global. ~~The authors~~ We expect that most of the ~~Dust~~ dust aerosol measured at each station would be regional, since it has a much larger aerodynamic mean diameter of 3.1 micrometers, leading to much faster deposition velocity. In any case, both species are

followed backward in time for 20 days, and residence times are attributed for all geographic grid cells. However, ~~we use~~ for
135 the inversion we use the residence times in each cell for the area between latitude -30° to 90° and longitude from -40° to 140°.

2.3 Tikhonov regularization

We are concerned with the solution of minimization problems of the form

$$min\|Ax - b\| \tag{1}$$

$x \epsilon R^n$ where $\|\|$ denotes the Euclidean norm, A ϵ R^{m*n} is an ill-conditioned matrix, and the data vector $b \epsilon R^m$ is contaminated
140 by an unknown error $e \epsilon R^m$ that may stem from measurement inaccuracies and discretization error (Park et al., 2018). Thus,
$b = b_{exact} + e$. We are interested in computing the solution x_{exact} of minimal Euclidean norm of the least-squares problem
with error-free data vector,

$$min\|Ax - b_{exact}\| \tag{2}$$

$x \epsilon R^n$ associated with (2). The desired solution x_{exact} will be referred to as the exact solution. Since b_{exact} is not known, we
145 seek to determine an approximation of x_{exact} by computing a suitable approximate solution of (2).

Due to the ill-conditioning of the matrix A and the error e in the data vector b, straightforward solution of the ~~least-~~ least
squares problem (2) generally does not give a meaningful approximation of x_{exact} . Therefore, the minimization problem of
equation (2) is commonly replaced by a penalized least-squares problem of the form

$$min \left\{ \|Ax - b\|^2 + \lambda^2 \|L(x - x_0)\|^2 \right\} \tag{3}$$

150 $x \epsilon R^n$

This replacement is known as Tikhonov regularization. The parameter $\lambda \geq 0$ is the regularization parameter that balances
the influence of the first term (the fidelity term) and the second term (the regularization term), which is determined by the
regularization matrix $L \epsilon R^{p*n}$. Here p is an arbitrary positive integer. x_0 represents our a priori knowledge on the solution.

The purpose of the regularization term is to damp undesired components of the minimal-norm least-squares solution of
155 (1). The minimization problem (3) is said to be in standard form when L is the identity matrix I, otherwise the minimization
problem is said to be in general form. We are interested in Tikhonov regularization in general form, because for a suitable
choice of regularization matrix $L \neq I$ the solution of (3) can be a much better approximation of x_{exact} than the solution of
(3) with $L = I$. A smooth solution is obtained when the L matrix requires that the difference between two neighboring cells is
minimum. In other words, when the regularization matrix L is the first-order discrete derivative operator, it imposes smoothness
160 on the solution (Donatelli and Reichel, 2014). In our particular case, each row of A matrix corresponds to FLEXPART model
sensitivity (residence time in each grid cell) for each filter measurement, and each column of A matrix corresponds to a specific
geographic grid cell sensitivity for all filter measurements. b corresponds to the actual species mass concentration for each filter,

while x is the emission flux from each geographic grid cell. In other words, we try to extract information associated to residence time in each grid cell for each filter measurement.

165   We expect that uncertainties associated with the $PM2.5$ measurements, chemical analysis, and PMF model application will also be attributed as unknown error e in the regularization term. Cavalli et al. (2016) report a positive sampling artifact of 0.4 to 2.8 $\mu g\ C/m^3$ for PM collection on quartz fiber filters corresponding to 14 - 70% of the total carbon collected. Viana et al. (2006) report that approximately 14% of the $PM2.5$ mass may result from the adsorption of gaseous organic and inorganic compounds onto the filter or the particles already collected on it (positive artifact). They also state that prolonged sampling

170   times may lead to greater negative artifacts (i.e. loss of semi-volatile organic compounds and of ammonium nitrate). The uncertainty of the XRF, EC/OC and IC measurements range between less than 10% (IC) and up to 20% (XRF) (Manousakas et al., 2017a; Panteliadis et al., 2015; Mantas et al., 2014; Vratolis et al., 2018). According to AIRUSE 2016 EU project final report (Deliverable B2.4~~), ,~~ (IDAEA, 2016; Amato et al., 2016; Diapouli et al., 2017)), PMF results standard error was estimated for the ~~Secondary Sulfate~~ secondary sulfate source to be below 10%, while the ~~Dust~~ dust source standard error

175   ranged from below 5% to 40% ($PM2.5$ filters). An overall uncertainty approximating 30% in the results obtained from the filter analysis and species concentration for each city is therefore expected.

When no a priori information is available, the assumption in the Tikhonov regularization equation is that x_0 is 0. We seek in our case a smooth solution, requesting that emission fluxes of neighboring cells have differences close to 0~~differences. Smaller differences are achieved when absolute emission fluxes values are small (closer to 0)~~, while at the same time the measured

180   concentrations are reconstructed by the solution. Solutions with small emission fluxes absolute values have smaller differences in neighboring cells than solutions with large emission fluxes absolute values. This imposes solutions with emission fluxes as small as possible, leading to the underestimation of measured values. The underestimation is relevant to how important ~~is~~ the regularization term in equation ~~3.~~ 3 is. A perfect fit between the measured and modeled data is achieved when the regularization parameter λ is equal to 0. As we mentioned in the previous paragraph, an overall uncertainty approximating 30% is expected.

185   In order to regularize such an uncertainty level a large regularization parameter λ is required, thus leading to a significant underestimation of the model results. We have to keep in mind that if λ is close to 0, we perfectly reconstruct the measured concentrations, which include a large error due to the ~~reasons mentioned earlier~~aforementioned reasons. As the inverse process is not linear, such an approach would result in very large errors in the estimation of emission fluxes in each grid cell.

A ~~Secondary Sulfate~~ secondary sulfate aerosol species was identified in 14 out of 16 cities in the study, and therefore the

190   two cities without this species (Ankara, Lisbon) were excluded from the analysis. In a small number of samples in the 14 cities included in the study, negative concentrations were identified. These samples were excluded from the dataset used in the Tikhonov regularization. Dust aerosol concentration was identified in 16 cities. Nevertheless, after the PSCF analysis for ~~Dust~~ dust aerosol, only 6 cities were included in the Tikhonov regularization dataset. That is because the PSCF analysis indicated that most of the ~~Dust~~ dust aerosol identified was of local origin (~~Dust~~ dust resuspension). Filter samples that had negative ~~Dust~~

195   dust concentrations were also excluded.

2.4 $L - curve$ **method**

Commonly, if only a single regularization parameter needs to be determined, the norms of model and residuals are plotted against one another ~~,~~ so as to give an $L - curve$. This name comes from the curve's characteristic shape, and the preferred regularization parameter is then chosen by identifying the "elbow" of the curve. The strategy is justified ~~based on~~ by the principle of Occam's razor, which advocates reliance on the simplest (in the present context, smallest) model that can explain observations (Valentine and Sambridge, 2018; Hansen, 1992).

2.5 **Potential source contribution function (PSCF)**

Twenty-day backward FLEXPART runs were used to acquire the residence time over each geographic cell for each measurement and for all stations. For each cell the PSCF ratio was calculated.

$$PSCF_{i,j} = weight_{i,j} * m_{i,j}/n_{i,j} \tag{4}$$

where $m_{i,j}$ is the sum of residence times (sensitivity) in a cell for concentrations higher than the 90th percentile and $n_{i,j}$ is the sum of residence times for all measurements. Indexes i,j correspond to latitude and longitude of each grid cell. $PSCF_{i,j}$ is the measure of probability of a grid cell ($1°$ x $1°$) to contribute to the concentration of the pollutant measured at the receptor site considered (Perrone et al., 2018). In order to acquire the weight factor used for each cell, total residence times in cells were divided in percentiles. The weight coefficients 0.25, 0.5 and 0.75 were used for cells with total residence times up to the 25th, 50th, 75th percentiles, respectively.

We apply the PSCF analysis for each measurement station and each aerosol species. The information that we use is the overall residence time for all filters in each station ($n_{i,j}$) and the overall residence times in each grid cell for the filter measurements with the highest ~~Secondary Sulfate or Dust~~ secondary sulfate or dust aerosol concentrations ($m_{i,j}$). In other words, we extract information from the sum of residence times for all filters and the sum of residence times for filters with the highest concentration (90th percentile). Grid cells with very small residence time may result in PSCF with high uncertainty in the apparent high value. For large values of $n_{i,j}$, there is more statistical stability in the calculated value. Thus, to reduce the effect of small values of $n_{i,j}$, an empirically determined weight matrix is multiplied ~~into the PSCF value~~ with the PSCF ratio to better reflect the uncertainty in the values for these cells (Polissar et al., 2001).

~~Twenty day~~ Twenty-day backward runs were used so as to assess species with high residence times in the atmosphere like Sahara dust.

3 Results and Discussion

3.1 Secondary ~~Sulfate~~ sulfate aerosol

The ~~Secondary Sulfate~~ secondary sulfate concentration identified in each station was simulated by an aerosol log-normal distribution with an aerodynamic geometric mean diameter of 400 nm and a standard deviation of 1.6. From each station the aerosol mass was released every 3 hours (within 4×10^4 discrete finite air masses) and followed backward in time for 20 days. The result obtained by FLEXPART was the residence time in each geographic cell. In Figure 2, the PSCF results for Zagreb, Athens, Krakow, Skopje, Vilnius, and Banja Luka are displayed. These cities were chosen as the areas indicated by their PSCF ~~corresponds~~ correspond to high emission fluxes according to emission maps (OMI-HTAP, ECLIPSE). In appendix A1 we display the PSCF results for the rest of the cities ~~that a Secondary Sulfate~~ for which a secondary sulfate concentration was identified.

In Figure 2, Athens indicates ~~as source areas~~ the center of the Balkans and Eastern Europe as source areas. Krakow points mainly to the area east of the Caspian Sea. ~~Banja Luka Secondary Sulfate~~ Banja-Luka's secondary sulfate main origin is the Volga region and Eastern Balkans. Vilnius~~Secondary Sulfate~~'s secondary sulfate comes from Ukraine and the Balkans. Skopje ~~Secondary Sulfate~~ secondary sulfate stems from the North of the Balkans and Northern Italy. A source area is also indicated in NW Africa. Zagreb indicates as source areas the Central and Eastern Balkans, the area around the Caspian Sea, and Asia Minor.

In 2 cities (Ankara, Lisbon), no ~~Secondary Sulfate~~ secondary sulfate concentration was indicated by the PMF analysis. Therefore 14 out of the 16 cities could be included, namely Tirana, Zagreb, Chisinau, Athens, Skopje, Debrecen, Banja-Luka, Sofia, Belgrade, Krakow, Montenegro, Kurchatov, Dushanbe, Vilnius (around 2,050 measurements). Our first approach was to apply the Tikhonov regularization to data from the 6 cities indicated by the PSCF analysis in Figure 2. Then we applied regularization to all 14 cities.

We applied the Tikhonov regularization to all 14 cities with an identified ~~Secondary Sulfate~~ secondary sulfate concentration, as we consider that ~~Secondary Sulfate~~ secondary sulfate and its precursor gases are emitted from many source areas in both Europe and Asia, and we needed as many stations and measurements as possible in order to identify them.

In Figure 3, the emission fluxes for ~~Secondary Sulfate~~ secondary sulfate aerosol calculated by the Tikhonov regularization method for 1° x 1° cells are presented. We used this resolution in the range of latitudes from -30° to 90° and longitude from -40° to 140°. This corresponds to a 120*160 (19,200 unknown factors) emission cell matrix, a number much higher than the total number of measurements. ~~We have~~ It is important to keep in mind that not all species are measured at all stations and even when a species exists at a station, it may not be present in all samples.

The result for the 6 cities (~~1069~~ 1,069 measurements) is depicted in Figure 3a, while the result for 14 cities is displayed in Figure 3b.

The SO_2 emission inventory of OMI-HTAP is also displayed in Figure 3c (Liu et al., 2018). It includes the non-energy emissions (from industry, residential and transportation) and the energy emissions. Note that aviation and shipping emissions are not included in the OMI-HTAP inventory. The high emission grid cells of the Tikhonov regularization solution for 14 cities
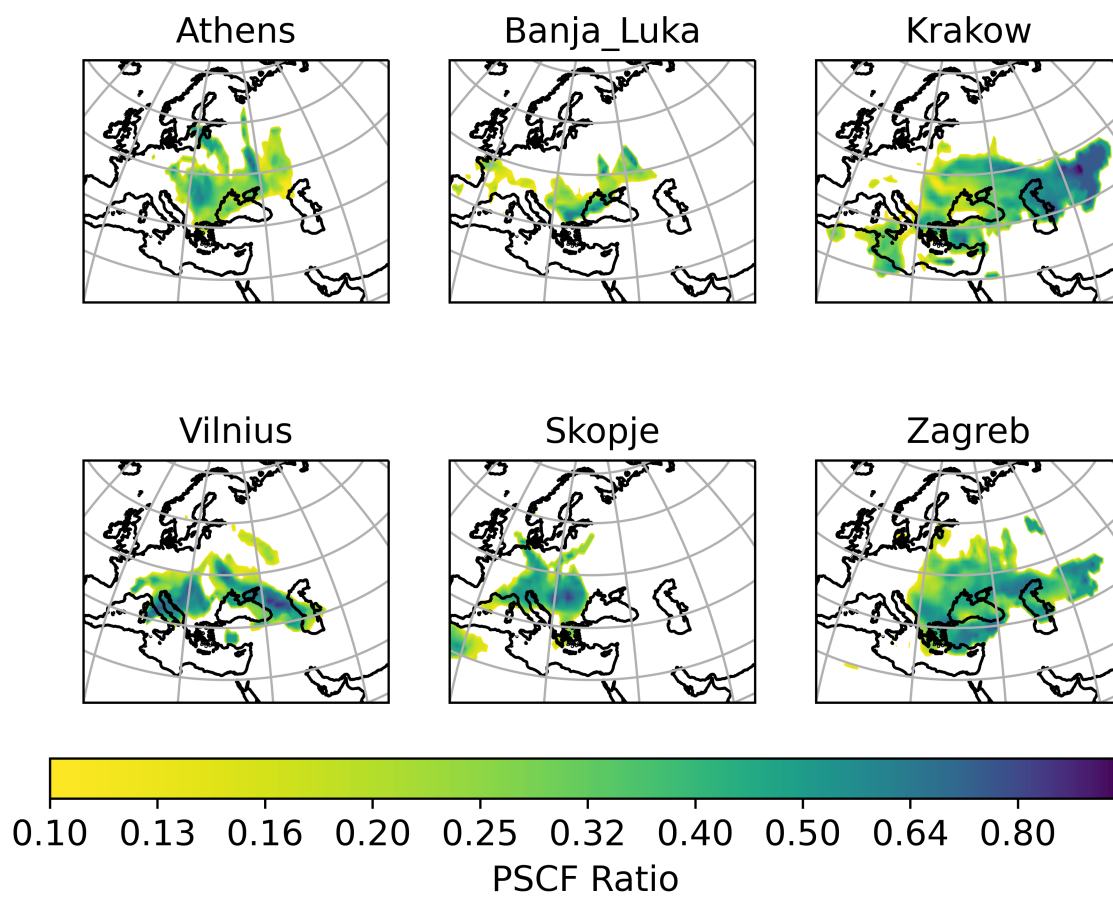
Figure 2. PSCF analysis ~~at~~ for concentrations higher than the 90th percentile ~~for Secondary Sulfate~~ of secondary sulfate aerosol, Zagreb, Athens, Vilnius, Krakow, Banja Luka, Skopje. The horizontal bar represents the PSCF ratio ($PSCF_{i,j} = weight_{i,j} * m_{i,j}/n_{i,j}$).

are indicated by shaded areas. We observe that there are high emission fluxes in the SO_2 OMI-HTAP map in the indicated areas.

We also observe in Figure 3 that the areas indicated by the Tikhonov regularization solution for 14 cities (Figure 3b), namely the Central and Western Balkans, South Poland and the area East of the Caspian Sea, are apparent also in the ECLIPSE SO_2 database map (Klimont et al., 2017). Again, we indicate these areas by adding an oval shade. ECLIPSE SO_2 database includes energy production, industry, oil and gas flaring, transport, shipping, agriculture, residential and waste emissions. As already mentioned earlier, a high level of uncertainty is expected in our input data. We excluded negative ~~Secondary Sulfate~~ secondary sulfate concentration measurements from the calculations, due to their high uncertainty. In Figure 3b, which corresponds to the solution for all available data (14 stations), the highest values are as follows:

For the area East of the Caspian Sea, the maximum value is $10 \times 10^{-12}\ kg*m^{-2}*s^{-1}$ for latitude 37°-38° North and longitude 67°-68° East. In the OMI-HTAP SO_2 map, the maximum value in the area is in latitude 39°-40° North and 65°-66° East, with a value of $7.7 \times 10^{-10}\ kg*m^{-2}*s^{-1}$.

For the area in the ~~west~~ West Balkans, the maximum value is $7.8 \times 10^{-12}\ kg*m^{-2}*s^{-1}$ for latitude 44°-45° degrees North and longitude 16°-17° East. In the OMI-HTAP SO_2 map, the maximum value in the area is in latitude 44°-45° North and 18°-19° East, with a value of $9.2 \times 10^{-10}\ kg*m^{-2}*s^{-1}$.

For the area in Poland, the maximum value is $6.1 \times 10^{-12}\ kg*m^{-2}*s^{-1}$ for latitude 49°-50° degrees North and longitude 19°-20° East. In the OMI-HTAP SO_2 map, the maximum value in the area is in latitude 51°-52° North and 19°-20° East, with a value of $5.3 \times 10^{-10}\ kg*m^{-2}*s^{-1}$.

For the area in the Central Balkans, the maximum value is $8.3 \times 10^{-12}\ kg*m^{-2}*s^{-1}$ for latitude 42°-43° North and longitude 20°-21° East. In the OMI-HTAP SO_2 map, the maximum value in the area is in latitude 44°-45° North and 18°-19° East, with a value of $9.3 \times 10^{-10}\ kg*m^{-2}*s^{-1}$.

In the solution for 6 cities (Figure 3a), very similar values to the ones for 14 cities were acquired in the areas of West and Central Balkans, Poland. We expect that the hotspot areas in the Tikhonov regularization solution are the most important for the transported ~~Secondary Sulfate~~ secondary sulfate for the cities in the study, even though the calculated emission flux values might differ from the ones in emission inventories.

We also produced two more emission flux results: One including only measurements from Zagreb (around 600 measurements), and one including all participating European cities except Vilnius (around 1,800 measurements). The first result is indicative of using a dataset from just one measurement station. In the second result we exclude Vilnius, Dushanbe and Kurchatov data. Dushanbe and Kurchatov are situated in a significant distance from other stations, out of the region of Europe. Vilnius on the other hand is on the edge of the area that is covered by European stations. This result was produced as we wish to evaluate if ~~by its use~~ we could predict ~~Secondary Sulfate~~ secondary sulfate concentration in Vilnius.

The result for Zagreb (Figure 4b), due to the small number of measurements (562 samples with positive ~~Secondary Sulfate~~ secondary sulfate source values) used in relation to 19,200 unknown factors, lacks specificity, indicating Poland and Eastern Europe in general as the main source area. Central and Western Balkans also have a high impact on Zagreb. We included the
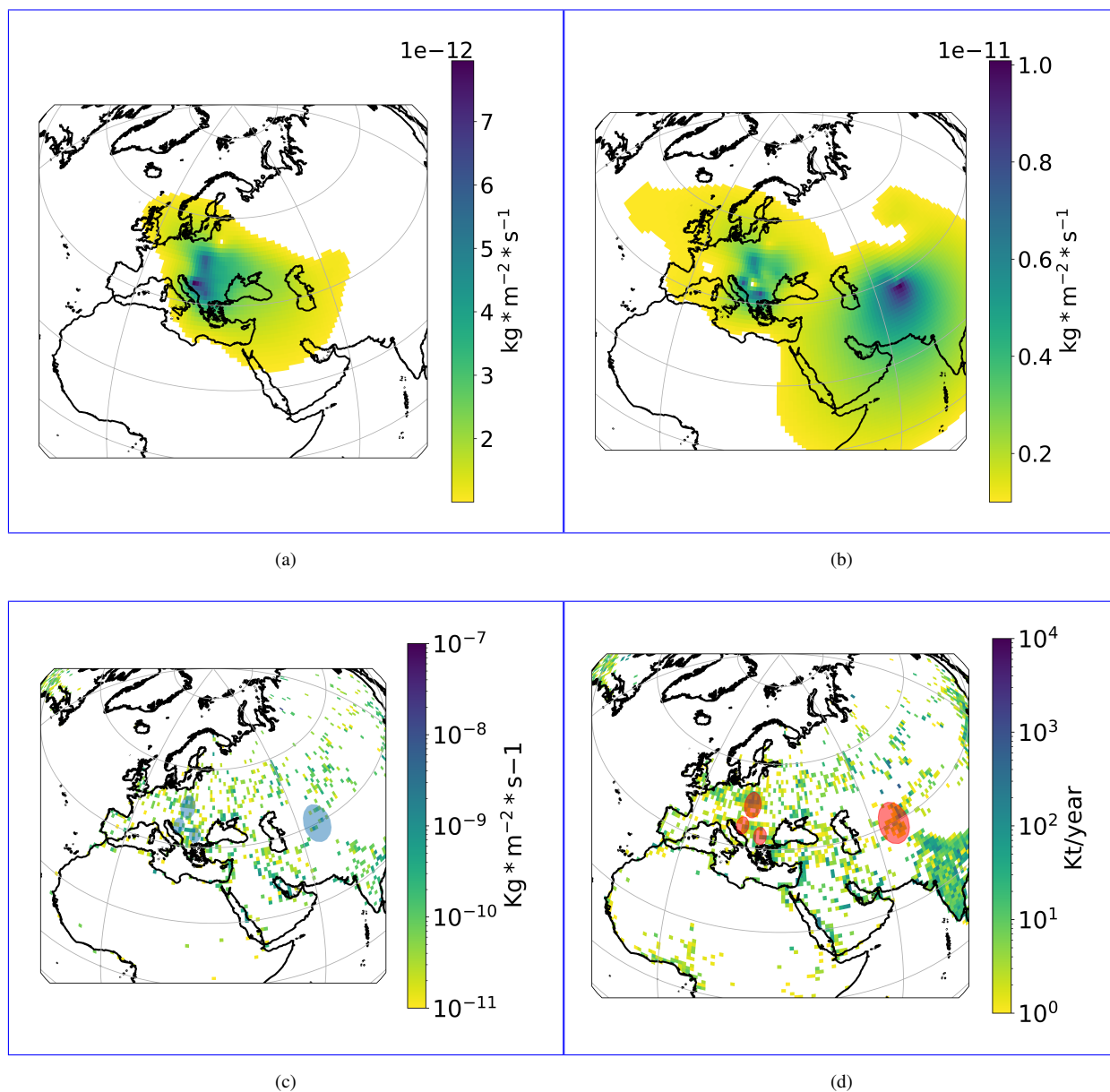
Figure 3. Secondary ~~Sulfate~~ sulfate aerosol Tikhonov regularization, $1°$ x $1°$ emission fluxes and OMI-HTAP, ECLIPSE emission maps. In subfigure (a) the solution for the 6 cities indicated by PSCF analysis (Zagreb, Athens, Vilnius, Krakow, Banja Luka, Skopje) is demonstrated. Subfigure (b) depicts the Tikhonov regularization emission fluxes solution when data from 14 stations are included. In subfigure (c) the OMI-HTAP emissions map during 2015 for SO_2 is demonstrated with units of $kg*m^{-2}*s^{-1}$. In subfigure (d) the ECLIPSE V6b database for SO_2 emissions during 2015 is presented with units of kt/yr. Grid cells attributed high emission fluxes by the Tikhonov regularization are indicated in the emission inventories maps by shaded areas.
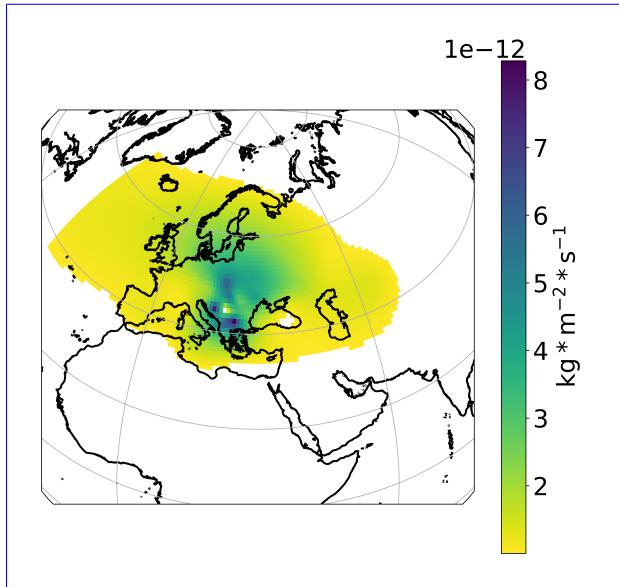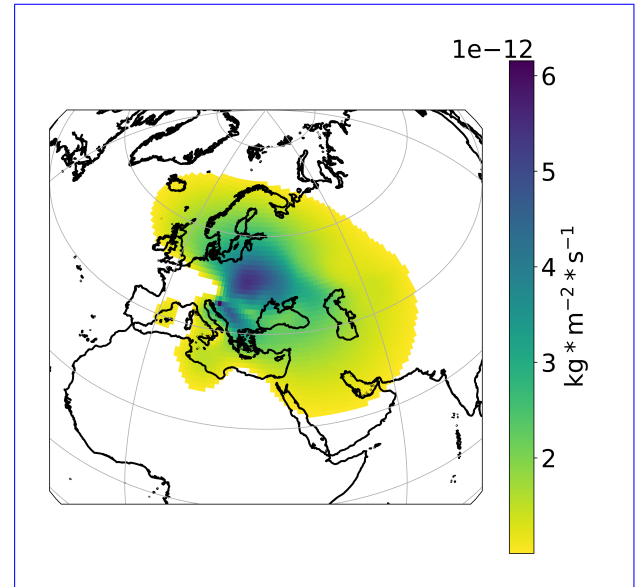
(a)   (b)

Figure 4. Secondary ~~Sulfate~~ sulfate aerosol Tikhonov regularization, $1°$ x $1°$ emission fluxes for (a) European stations excluding Vilnius (Athens, Banja-Luka, Belgrade, Chisinau, Debrecen, Niksic, Skopje, Sofia, Tirana, Krakow, and Lisbon), (b) Zagreb. The vertical bar corresponds to the emission fluxes of secondary sulfate aerosol from each geographic grid cell in $kg * m^{-2} * s^{-1}$.
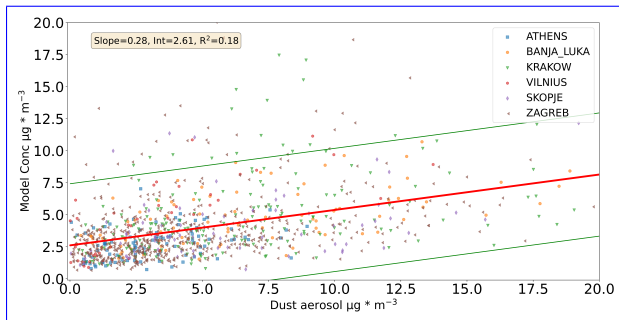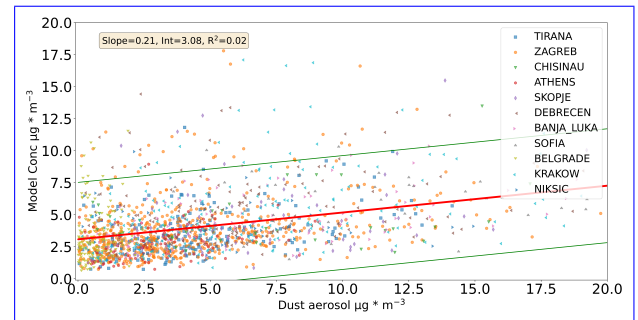
(a)   (b)

Figure 5. Comparison between the measured ~~Secondary Sulfate~~ secondary sulfate and the ~~Modeled~~ modeled values based on the Tikhonov regularization solution for 6 cities in (a), and 14 ~~stations~~cities in (b). Regression line $\pm$ 2 standard deviations is also depicted. The legend presents the measurement location.

290 emission flux results for Zagreb as it was the station with the largest number of filter samples ~~that participated~~ in the study. This case represents the results we could expect when we use data from a single station.

When we compare the OMI-HTAP emission map for SO_2 (Liu et al., 2018) to the emission map acquired by the Tikhonov regularization for the investigated European cities excluding Vilnius (Figure 4a), we observe many similarities. The hotspots in Balkans and South Poland are apparent in both maps.

295 We also find similarities between the PSCF analysis (Figure 2) and the regularization result when 14 cities are included. In particular, the area ~~east~~ East of the Caspian Sea appears to contribute significantly in the PSCF performed for Zagreb and Krakow, as well as in the Tikhonov regularization solution.

The PSCF result for Dushanbe (Figure A.1) indicates the ~~areas east~~ area East and SE of the Caspian Sea as potential sources. This is also apparent in the solution when we include all stations and the OMI-HTAP emission map for SO_2. Central Asia,
300 comprising Kazakhstan, Kyrgyzstan, Tajikistan, Uzbekistan and Turkmenistan, has developed rapidly in terms of population, industrialization and urbanization over the past few decades, accompanied by increased anthropogenic emissions. These emissions, along with regional and local dust, are often subject to long-range atmospheric transport by westerlies toward the Tian Shan and the Tibetian plateau. Biomass burning is a significant contributor to primary organic carbon emissions (Chen et al., 2022).

305 The center of the Balkans appears as a source area according to the PSCF for Zagreb and Athens, as well as the Tikhonov regularization solution for 14 cities (Figure 3b).

In the Tikhonov regularization result for the 6 cities (Figure 3a), resulting emission fluxes for all grid cells were positive. In the other 3 Tikhonov regularization results (Figures 3b, 4a, 4b), we allowed for small negative emission fluxes (-5×10^{-13} $kg * m^{-2} * s^{-1}$).

310 When we compare the modeled concentrations for ~~Secondary Sulfate~~ secondary sulfate using the solution for 14 cities to measured values at each station (Figure 5b), the agreement is not good. This is probably due to uncertainties associated with the data, the influence of the regularization term in equation 3 and the lack of a priori information, as explained in section 2.3 (Tikhonov regularization). In Figure 5b, the intercept is 3 $\mu g * m^{-3}$ and the slope is close to 0.3.

The modeled concentration was acquired according to equation 5, following (Pisso et al., 2019).

$$Model\ Conc\ (kg*m^{-3}) = \sum_{lat=-30°}^{90°} \sum_{lon=-40°}^{140°} (residence\ time_{i,j}(s) * x_{exact-i,j}(kg*m^{-2}*s^{-1})/height\ of\ 500\ m) \quad (5)$$

In Figure A.4 (appendix) we present the emission fluxes Tikhonov regularization solution (14 cities) for ~~Secondary Sulfate~~ secondary sulfate aerosol during summer (April to September) and winter (October to March) months. In winter, as expected, emission fluxes have significantly higher values than summer. In summer the hotspot ~~east~~ East of the Caspian Sea almost disappears, indicating that these emissions probably relate to heating. In South Poland the hotspot is significantly reduced.
320 Hotspots on Western and Central Balkans appear to have similar values in winter and summer, indicating that they possibly originate from power plants.
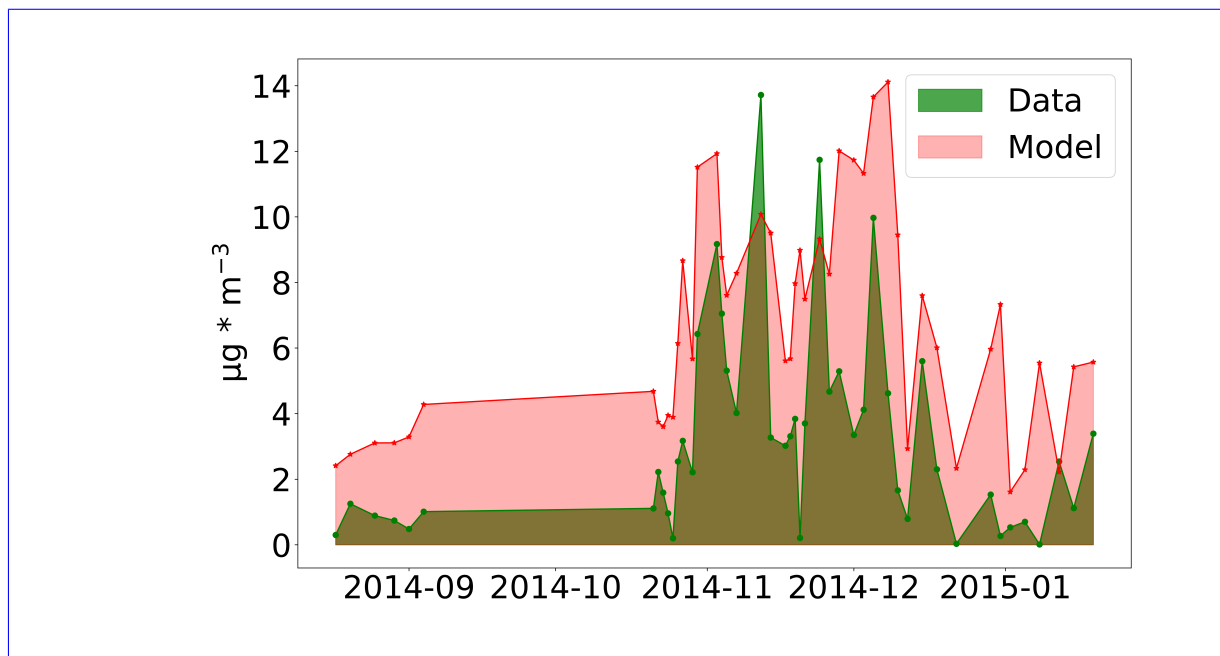
(a)

Figure 6. Comparison of modeled and measured ~~Secondary Sulfate~~ secondary sulfate aerosol concentration at Vilnius. The emission fluxes solution used is the one acquired by Tikhonov regularization when Vilnius, Dushanbe, Kurchatov data are excluded (data from Athens, Banja-Luka, Belgrade, Chisinau, Debrecen, Niksic, Skopje, Sofia, Tirana, Krakow and Lisbon).

3.1.1 The case of Vilnius

In Figure 6, we compare the modeled and measured ~~Secondary Sulfate~~ secondary sulfate aerosol concentration at Vilnius with the 1-degree resolution model. We used the result of the Tikhonov regularization when we excluded the data from Vilnius, Dushanbe and Kurchatov to acquire the modeled values.

In general, the agreement between the modeled and the measurement data ~~are~~ is relatively good. The agreement is not good for very low measured concentration values of ~~Secondary Sulfate~~secondary sulfate. The lowest $PM2.5$ concentrations in the dataset are observed during August, September, until nearly the end of October. This could also be related to the beginning of the winter season, with increased emissions due to heating.

Vilnius station was chosen for the demonstration of the results as it is situated on the edge of the area that the rest of the European stations of the study cover.

3.2 Dust aerosol

The first step in order to identify potential source areas was to apply the PSCF analysis on all cities. Meaningful results, in the sense that the indicated potential source areas do indeed emit ~~Dust~~ dust aerosol, were acquired only in the cases of Athens,
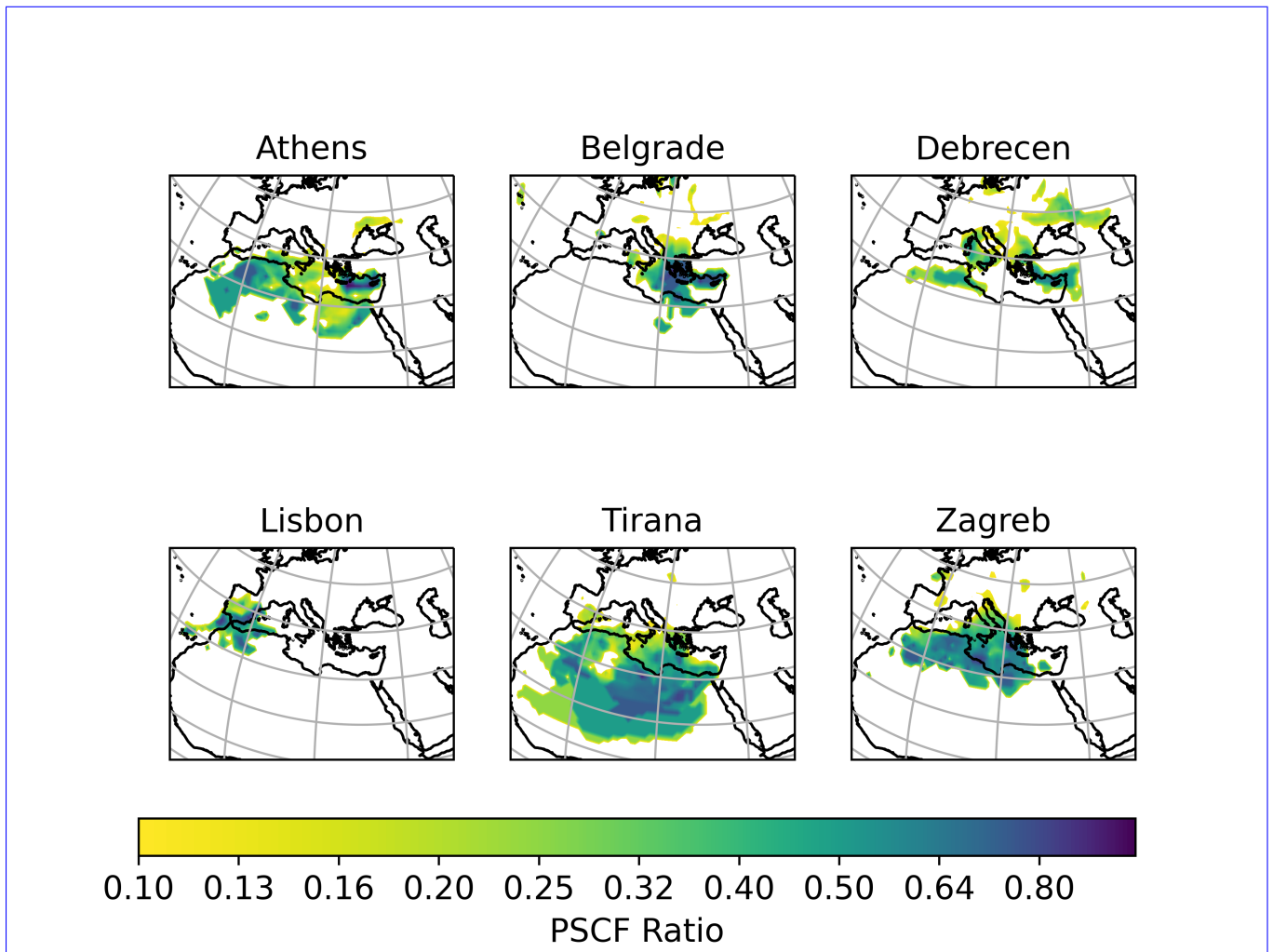
Figure 7. PSCF analysis ~~at~~ for concentrations higher than the 90th percentile ~~for Dust~~ of dust aerosol, Athens, Belgrade, Debrecen, Lisbon, Tirana, Zagreb. The horizontal bar represents the PSCF ratio ($PSCF_{i,j} = weight_{i,j} * m_{i,j}/n_{i,j}$).

335 Belgrade, Debrecen, Lisbon, Tirana and Zagreb. In Figure 7 the PSCF results at the 90th percentile for ~~Dust~~ dust aerosol for these stations are displayed. Potential source areas for Athens were North Africa and the Middle East, for Belgrade NE Africa and the Middle East, for Debrecen Western Africa and the Middle East, for Lisbon Western Africa, for Tirana North Africa and for Zagreb North Africa. The PSCF results for the rest of the stations (Ankara, Dushanbe, Vilnius, Krakow, Kurchatov, Banja-Luka, Chisinau, Niksic, Skopje, Sofia) indicated that their ~~Dust~~ dust aerosol was mainly of local origin (~~Dust re-suspension~~ dust

340 resuspension, please refer to Figures A.6, A.7 in the appendix).

In the second step, in order to quantify the ~~Dust~~ dust aerosol emitted from each geographic grid cell, the Tikhonov regularization was applied to the data from Athens, Belgrade, Debrecen, Lisbon, Tirana, and Zagreb, excluding negative values (1,320 measurements were used).

In Figure 7 the PSCF for the 90th percentile for ~~Dust~~ dust aerosol is presented. ~~For~~ In the PSCF subfigure for Tirana two paths can be seen: In the first path, winds from the Atlantic Ocean pass over NW Africa, then the Mediterranean Sea and subsequently reaching Tirana. In the second path, winds from the Atlantic Ocean pass over NW Africa, then NE Africa and the Mediterranean Sea, subsequently reaching Tirana. The second path is by far the prevailing one for the 90th percentile highest concentrations of ~~Dust~~ dust aerosol for Tirana, as can be seen in Figure A.3 in the appendix. ~~Please~~ It is important to keep in mind that the residence times depicted correspond to a height up to 500 m so as to always be within the boundary layer. Therefore, while the ~~Dust~~ dust load could be mainly picked up in both cases in NW Africa, due to longer residence times in NE Africa, this area could appear as the most probable to be the one that emits ~~Dust~~ dust aerosol. This could be partly due to the fact that as the air masses travel over Africa at low altitude, wind speed is reducing due to higher friction over land in comparison to when they travel over the ~~Sea~~ sea (Atlantic or Mediterranean). The air masses probably have higher speed over NW Africa and this results in more dust being picked up in this area. Some ~~Dust~~ dust aerosol could be picked up from NE Africa and its origin could also be the Arabian Peninsula. This path is also evident in Figure 8, where a weak emission area is indicated in the NE Africa.

While for the PSCF analysis ~~,~~ Tirana, Zagreb, and Belgrade indicate high probability for NE Africa to be a source area, this is not the case for the Tikhonov regularization result. In Figure 8, the result indicates that NW Africa is by far the most significant ~~Dust~~ dust aerosol source area for the 6 cities (Athens, Belgrade, Debrecen, Lisbon, Tirana, and Zagreb) whose data we used. NE Africa also has a hotspot in Figure 8, but its contribution was significantly lower when the data from these 6 stations are combined. In the borders between Mauritania, Algeria and Mali, the highest emission fluxes are identified (lat 27° N, long -4° E), which are as high as $17.6 \times 10^{-12}\ kg * m^{-2} * s^{-1}$.

Stohl et al. (2009), referring to halocarbons, state that inaccuracies in model and data will in general cause their method to find solutions containing unrealistic negative emissions that are larger than expected. In the linear framework this cannot be prevented directly as positive definiteness is a nonlinear constraint. They also suggest an iteration method so as the sum of all negative emissions is less than 3‰ of the sum of the positive emissions. In our case with the ~~Dust~~ dust aerosol we allow small negative emission values $(-2.5 \times 10^{-12}\ kg * m^{-2} * s^{-1})$ representing higher deposition velocities than calculated by the FLEXPART deposition scheme.

In Figure 9 the comparison between the modeled data using the Tikhonov regularization solution for ~~Dust~~ dust and measured concentrations is presented. In this case we have a small intercept, but still the measured concentration is underestimated by the modeled values.
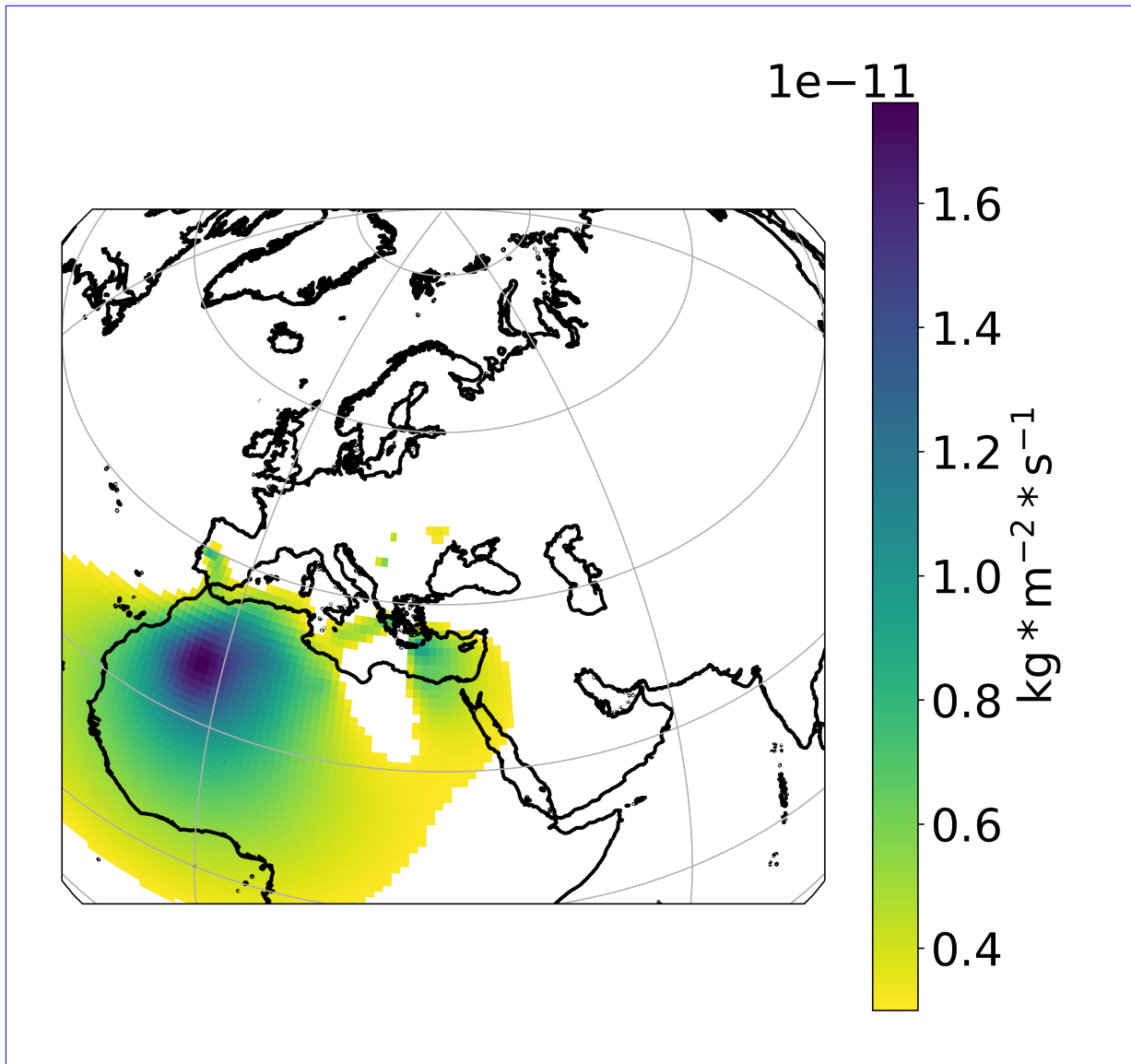
Figure 8. Dust aerosol Tikhonov regularization, $1° \times 1°$ emission fluxes for data from Athens, Belgrade, Debrecen, Lisbon, Tirana, and Zagreb. The vertical bar corresponds to the emission fluxes of dust aerosol from each geographic grid cell in $kg * m^{-2} * s^{-1}$. The main source area depicted is NW Africa.
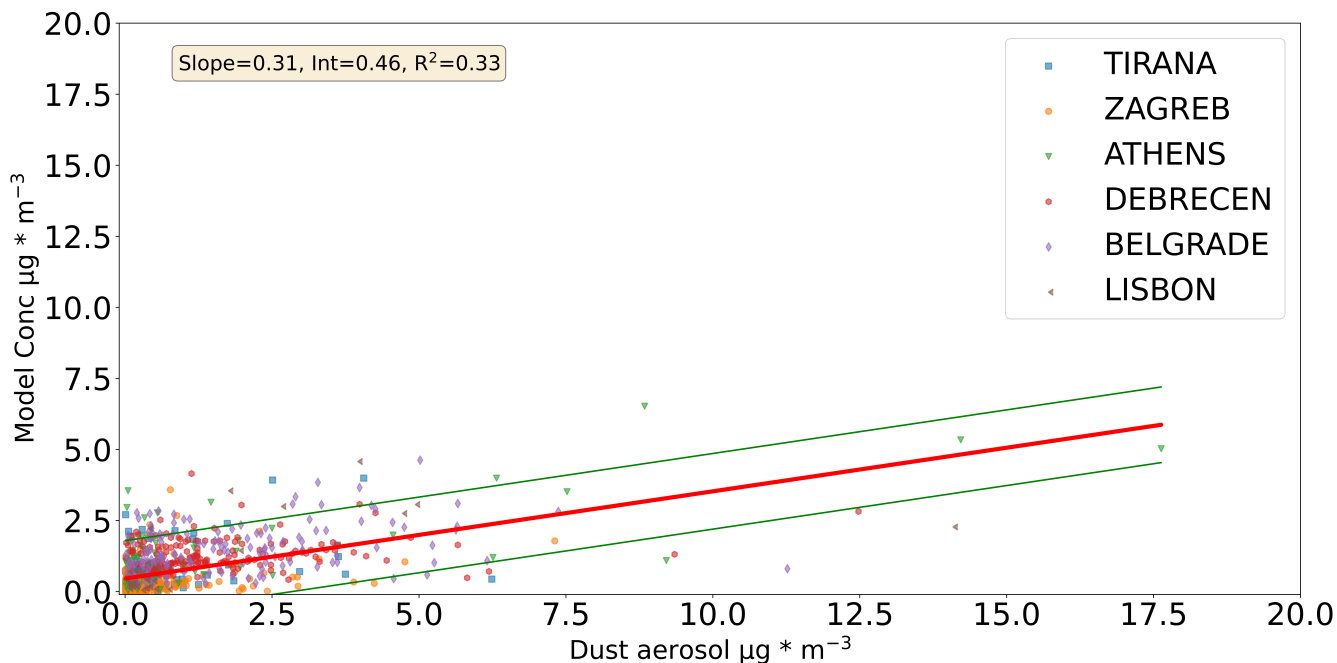
Figure 9. Comparison between the measured ~~Dust~~ dust concentration and the ~~Modeled~~ modeled values based on the Tikhonov regularization solution for Athens, Belgrade, Debrecen, Lisbon, Tirana, and Zagreb. Regression line $\pm$ 2 standard deviations is depicted. The measurement location is provided in the legend.

4   Summary and Conclusions

Emission fluxes of ~~Secondary Sulfate and Dust~~ secondary sulfate and dust aerosol were identified and their transport contri-bution was quantified based on a dataset including measurements from 16 cities in Europe and Asia. In the ~~Secondary Sulfate case~~ secondary sulfate case, 14 out of the 16 cities were used, as only in those a ~~Secondary Sulfate~~ secondary sulfate aerosol species was identified through PMF analysis. In the ~~Dust aerosol case~~ dust aerosol case, 6 cities were used as in the rest of the cities, based on PSCF analysis, ~~Dust~~ dust aerosol was considered to be of local origin. There was one city whose results were not used at all (Ankara) and one city whose results were used only for ~~Dust~~ dust aerosol (Lisbon). Data from Chisinau, Skopje, Banja-Luka, Sofia, Belgrade, Montenegro, Kurchatov, Dushanbe, and Vilnius were only used for the ~~Secondary Sulfate~~ secondary sulfate aerosol case.

For ~~Secondary Sulfate~~ secondary sulfate, in the case that data from 14 stations were incorporated, the highest emission fluxes for Europe were found to be in Poland, Eastern Europe, Central and Western Balkans. In Asia, the NE area of the Caspian Sea had the maximum emission flux. Its value was as high as $10 \times 10^{-12} \, kg * m^{-2} * s^{-1}$.

The produced emission fluxes solutions for ~~Secondary Sulfate~~ secondary sulfate are evaluated by comparison to existing emission maps. The hotspots indicated by the Tikhonov regularization method appear to have high emission fluxes for OMI-

HTAP and ECLIPSE SO_2 inventories. The Tikhonov regularization solutions for secondary sulfate do not cover the multiple significant source areas depicted in emission inventories. This probably relates to the fact that we do not have enough information with the stations and measurements at hand so as to have a high resolution result. However, we expect that hotspot areas in the Tikhonov regularization solution are the main areas whose emissions influence the cities in the study.

When the secondary sulfate regularization solution for European cities excluding Vilnius was applied (data from 11 cities, we excluded Vilnius, Dushanbe, Kurchatov) to aerosol masses originating from Vilnius, a relatively good agreement was found between the modeled and the measured values. This indicates the robustness of the method, as we can acquire a useful approximation to the concentration of any station for an aerosol species that is mainly transported, based only on measurements conducted in the greater geographic area. That holds even for secondary sulfate, an aerosol component that is not emitted as such, but is produced in the atmosphere from precursor gases several hours after their release.

The main source area of dust aerosol for Athens, Belgrade, Debrecen, Lisbon, Tirana, and Zagreb was NW Africa (Sahara dust). There was also evident contribution from the NE Africa, but significantly lower. The maximum emission flux was as high as $17.6 \times 10^{-12} \ kg * m^{-2} * s^{-1}$.

The result by the Tikhonov regularization for dust indicates NW Africa as the most significant source area, while the PSCF results for dust (Figure 7) demonstrate high probability for NE Africa to be a source area too. We consider that the Tikhonov regularization result is more reliable, since wind speed is expected to be higher in NW Africa, and therefore more dust aerosol will be picked up by air masses there.

An overall good agreement between the measured and modeled concentrations for participating cities is not achieved. It should be noted that the result for dust is better than the result for secondary sulfate, as it has much smaller intercept and higher coefficient of determination (R^2) (Figures 5 and 9). This is probably due to the fact that the secondary sulfate concentration depends also on atmospheric chemistry.

The purpose of the development of the new method was to contribute to the air quality management process. With this new method, an improved identification of source areas for the long range transported aerosol in comparison to PSCF analysis is achieved. Also, the relative importance of emission fluxes from each geographic grid cell is classified. This classification could be compared to existing emission inventories, resulting in possible improvements in the emission fluxes calculation algorithms. The new method also provides an estimate of the magnitude of emission fluxes from each grid cell. For secondary sulfate, around 60% of the measured concentrations magnitude could be reconstructed (Figure A8a) based on the deducted emission fluxes, while for dust, approximately 45% could be reconstructed (Figure A8b). This indicates that in this case, the new method significantly underestimates emission fluxes and measured concentrations. It is important to keep in mind though that if data with lower uncertainty are used, the underestimation would be significantly lower. Also, additional a priori information could lead to better performance of the method. Since we identify the pollutant source area, its relative magnitude and acquire an estimate of the measured concentrations, we can implement targeted mitigation measures. This approach can be used for any pollutant that can be simulated in FLEXPART or any similar model, without the need of an emission inventory. Ideally, we would like to implement the new method in combination to chemical transport models, so as to improve mitigation measures estimation. We should keep in mind that the emission fluxes

deducted by the new method are averages over a period of 3 years. Emission fluxes have seasonal, monthly, weekday and daily variations in each geographic grid cell. Therefore, the emission fluxes result derived by Tikhonov regularization can only approximate roughly the concentrations measured at the cities participating in the study. Nevertheless, we still have enough information so as to plan mitigation measures.

425   Further work could include the application of the new method on other aerosol components, like Black Carbon, so as to estimate its emission fluxes from each geographic grid cell.

Code availability.   Code will be available upon request

Data availability.   The data files used to produce the results are deposited at Zenodo:

    Stergios Vratolis, Evangelia Diapouli, Manousos I. Manousakas, Susana Marta Almeida, Ivan Beslic, Zsofia Kertesz, Lucyna Samek, &
430 Konstantinos Eleftheriadis. (2023). A new method for the quantification of ambient particulate matter emission fluxes - Data [Data set]. Zenodo. https://doi.org/10.5281/zenodo.7912793

Appendix A: Results

A1   Secondary ~~Sulfate~~ sulfate PSCF, cities not included in Figure 2

Dushanbe indicates the area East of the Caspian Sea (NE and SE) as source. Belgrade ~~Secondary Sulfate~~ secondary sulfate
435 mainly stems from the Eastern Mediterranean. Chisinau indicates as source the South Balkans and Poland. It also indicates the area in the NE of the Caspian Sea. Debrecen ~~Secondary Sulfate~~ secondary sulfate also stems from the Eastern Mediterranean.

    We only have 50 measurements from Niksic and its PSCF results are not considered statistically significant. From Sofia we only have 50 measurements, clearly not enough for PSCF analysis. Tirana indicates a transport path from Ukraine and Central Europe. Kurchatov indicates ~~Secondary Sulfate~~ secondary sulfate source areas in Siberia, probably related to gas flaring.

440 ### A2   Footprint Tirana

In Figure A.3 the residence time ~~(sensitivity~~ in each grid cell (sensitivity of measurement station to emissions from each grid cell) for a height up to 500 m is displayed.

A3   Secondary ~~Sulfate~~ sulfate Tikhonov regularization solutions for summer - winter, 14 cities

We observe in Figures A.4 and A.5 that ~~Secondary Sulfate~~ secondary sulfate aerosol in Dushanbe has significantly higher
445 values in the winter, indicating influence from domestic heating. In Figure A.4 we ~~observe also~~ also observe that the hotspot over Poland is reduced in summer. The other source areas indicate similar values in winter and summer.
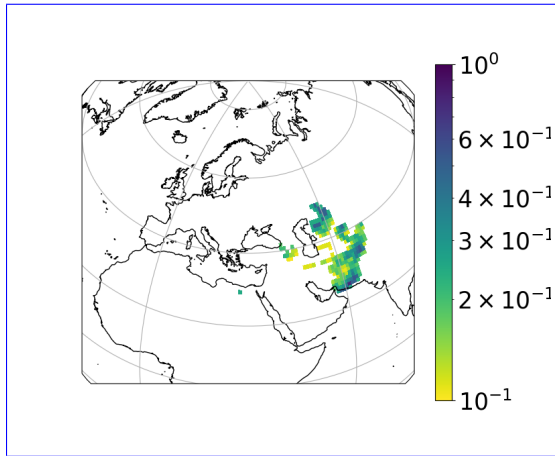
(a) Dushanbe
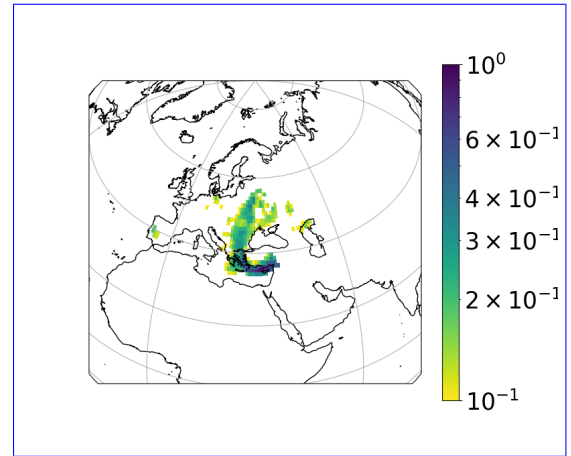
(b) Belgrade
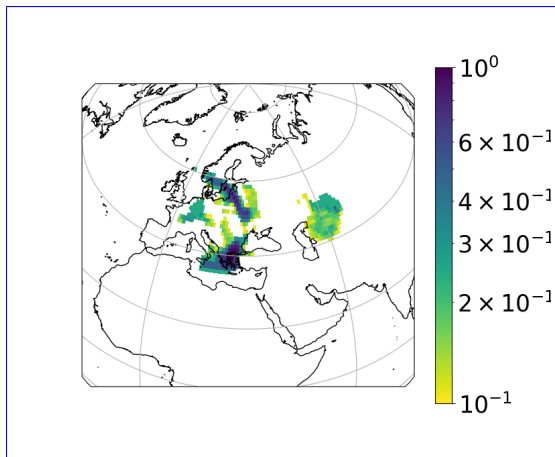
(c) Chisinau
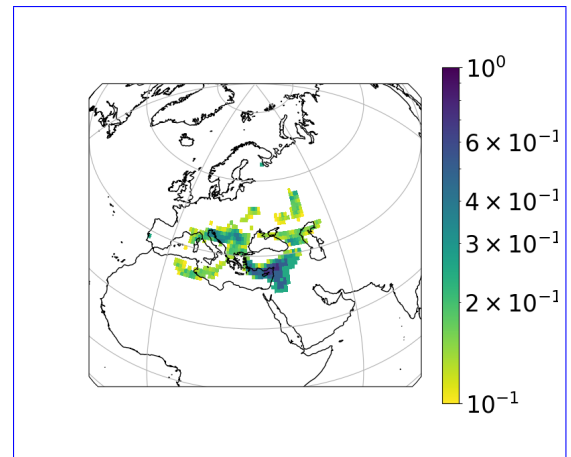
(d) Debrecen

Figure A1. PSCF analysis for ~~Secondary Sulfate~~ secondary sulfate aerosol for concentrations higher than the 90th percentile, Dushanbe, Belgrade, Chisinau, Debrecen. The vertical bar represents the PSCF ratio ($PSCF_{i,j} = weight_{i,j} * m_{i,j}/n_{i,j}$).
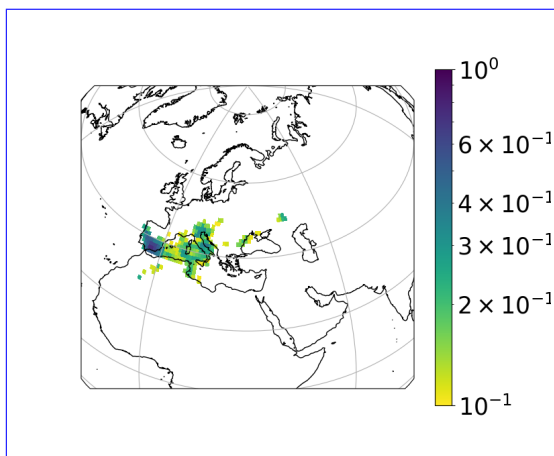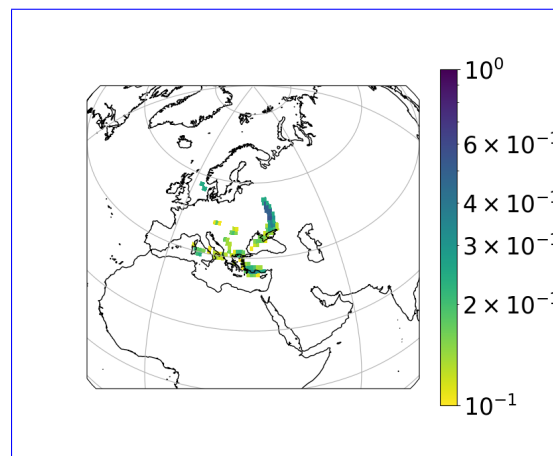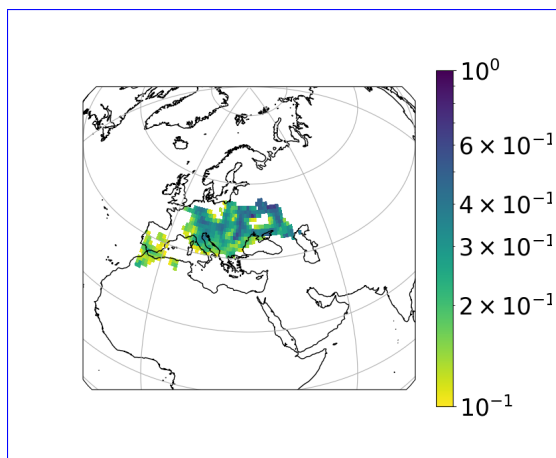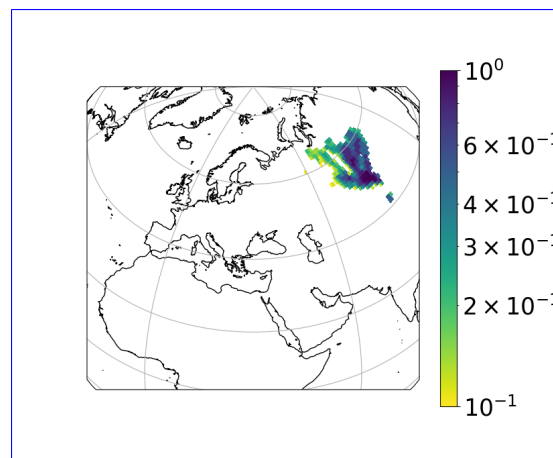
Figure A2. PSCF ~~analysis~~ for ~~Secondary Sulfate~~ secondary sulfate aerosol for concentrations higher than the 90th percentile, Niksic, Sofia, Tirana, Kurchatov. The vertical bar represents the PSCF ratio ($PSCF_{i,j} = weight_{i,j} * m_{i,j}/n_{i,j}$).
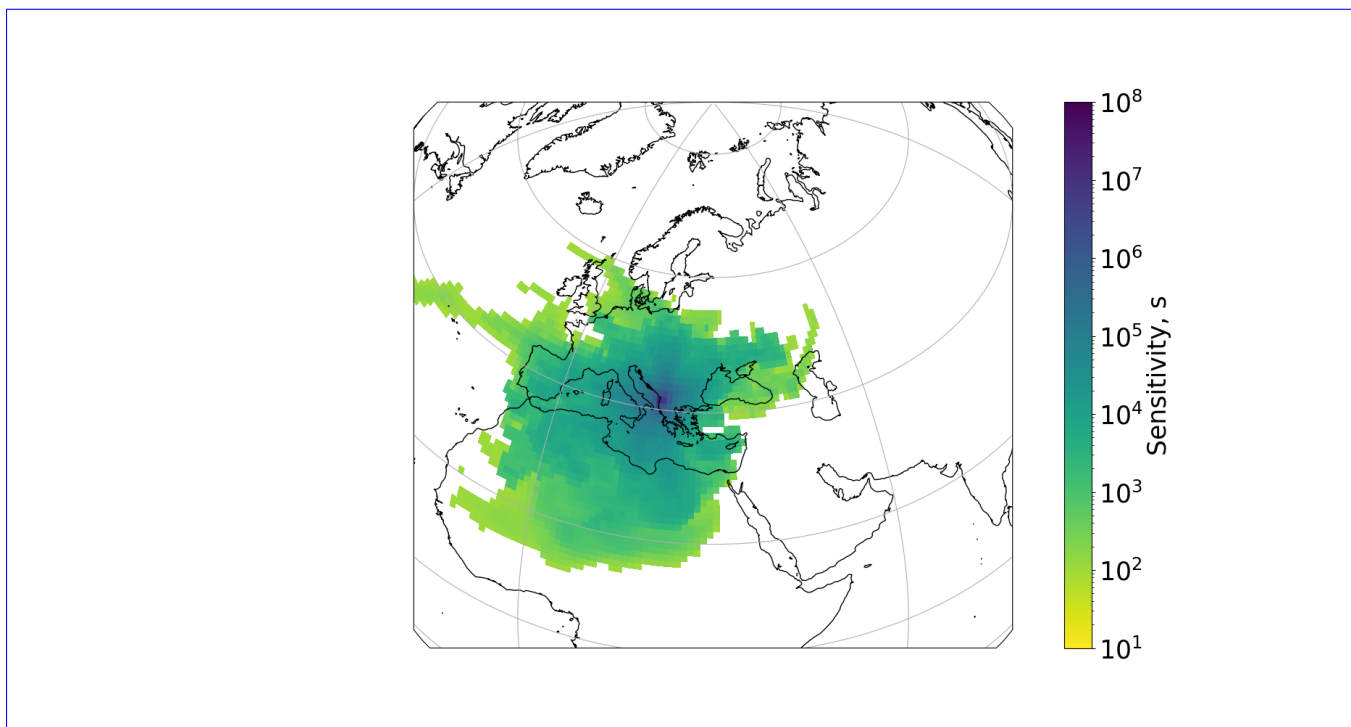
Figure A3. Tirana ~~Footprint~~residence time in each geographic grid cell for secondary sulfate aerosol, ~~s~~all filter measurements. The vertical bar corresponds to seconds residence time (sensitivity of measurement station to emissions from each grid cell). Air mass transport up to a height of 500 m agl is included.

A4 Dust PSCF, cities not included in Figure 7

In Figures A.6, A.7 we observe that the PSCF analysis at the 90th percentile ~~do~~ does not indicate high emission areas for ~~Dust~~ dust aerosol.

450 ## A5 Comparison between measured and modeled values for ~~Secondary Sulfate~~ secondary sulfate and ~~Dust~~ dust aerosol, no intercept

Author contributions. SV analysed data, interpreted results, prepared the figures and wrote the text of the manuscript. LD, MM, MA, IB, ZK, LS provided the PMF analysis data and contributed in interpreting results. KE contributed in interpreting results. All authors reviewed the final manuscript.

455 *Competing interests.* The authors declare that they have no conflict of interest.

(a) Summer (b) Winter
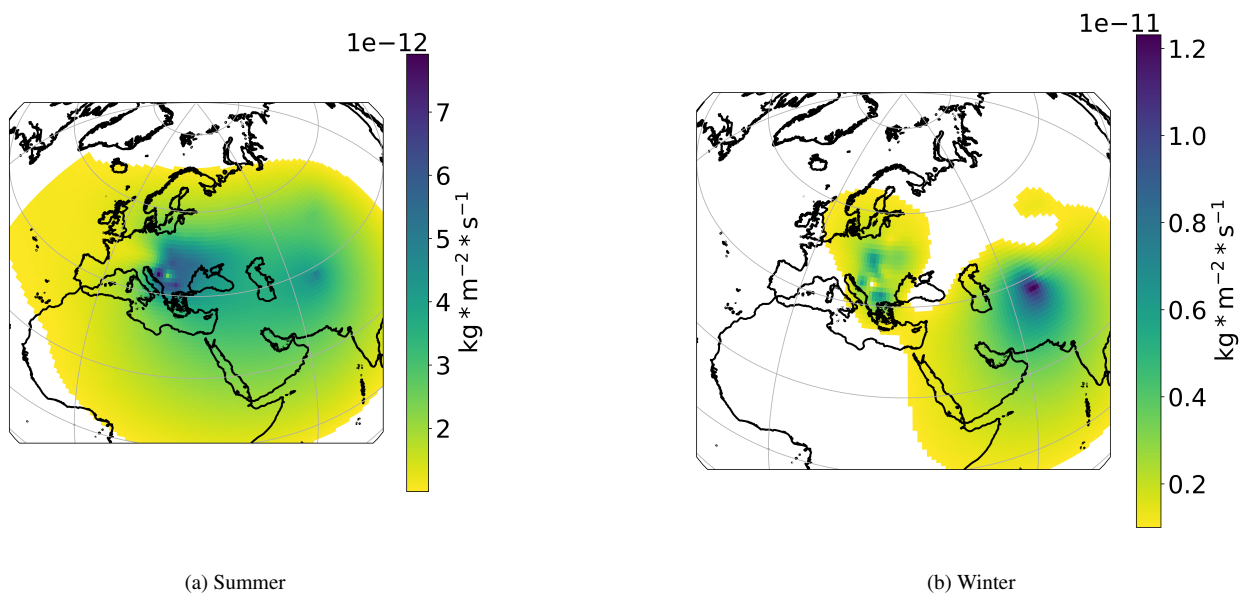
Figure A4. ~~Secondary sulfate~~ Tikhonov regularization ~~for Secondary Sulfate~~ solution for 14 ~~stations~~cities (emission fluxes), summer (April to September) and winter (October to March) months. The vertical bar represents the emission fluxes from each geographic grid cell in $kg * m^{-2} * s^{-1}$.

(a) Summer (b) Winter
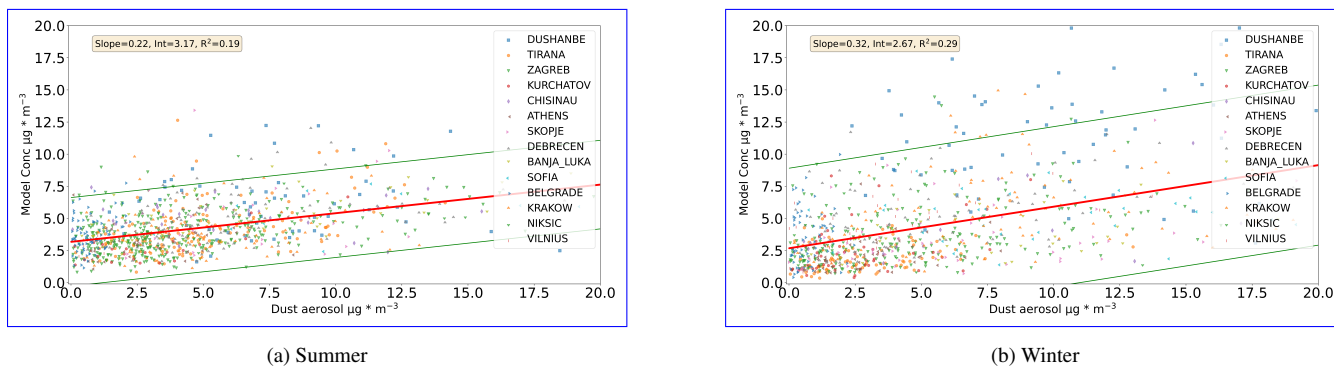
Figure A5. Comparison between modeled and measured ~~Secondary Sulfate~~ secondary sulfate aerosol concentration in summer (April to September) and winter (October to March) months. Regression line $\pm$ 2 standard deviations is depicted. The measurement location is presented in the legend.
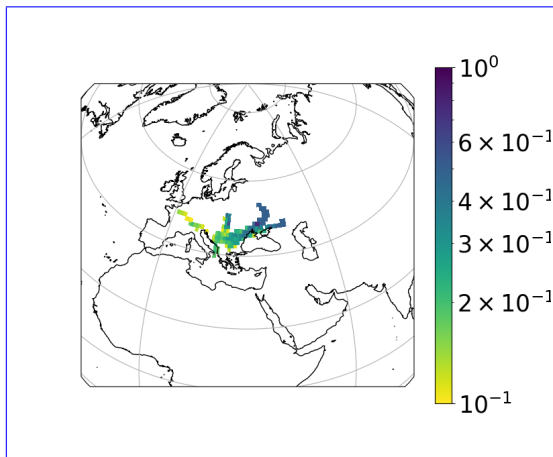
(a) Banja-Luka
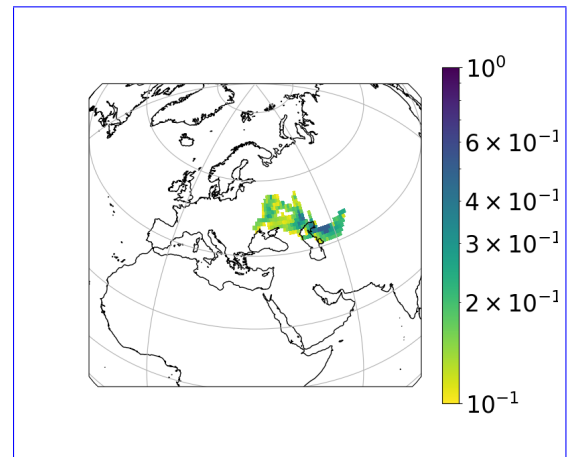
(b) Chisinau
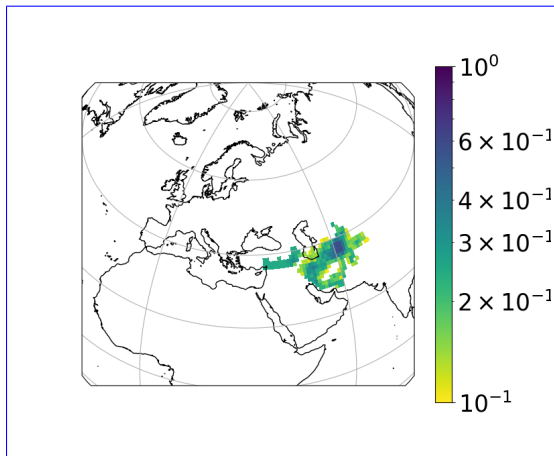
(c) Dushanbe
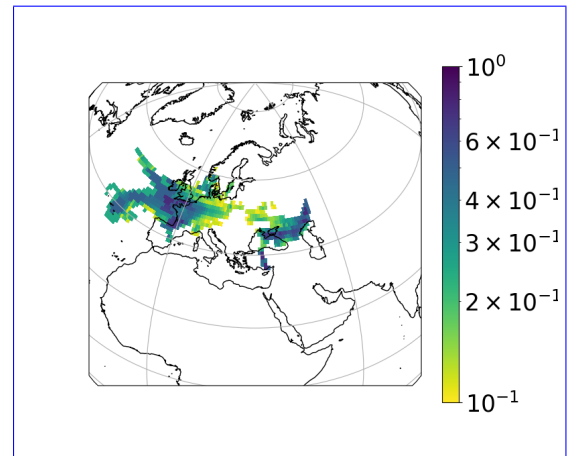
(d) Krakow
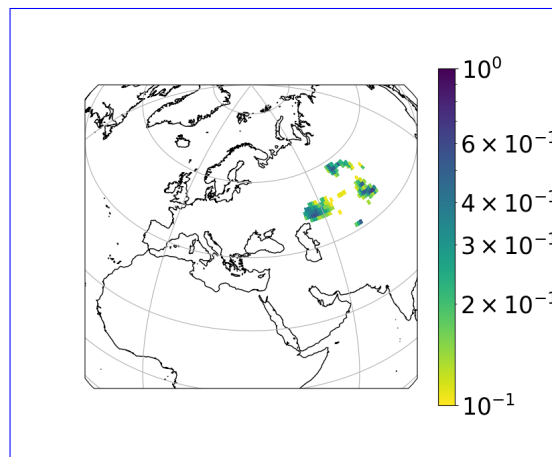
(e) Kurchatov

Figure A6. PSCF for ~~Dust~~ concentrations higher than the 90th per**26**ntile for dust aerosol ~~,~~ and for cities not included in Figure ~~7~~7. The vertical bar represents the PSCF ratio ($PSCF_{i,j} = weight_{i,j} * m_{i,j}/n_{i,j}$).
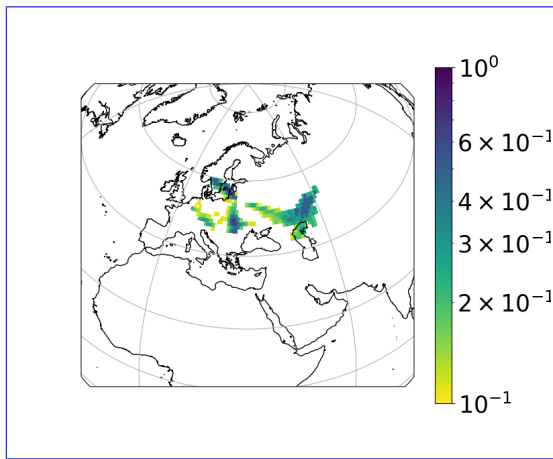
(a) Vilnius
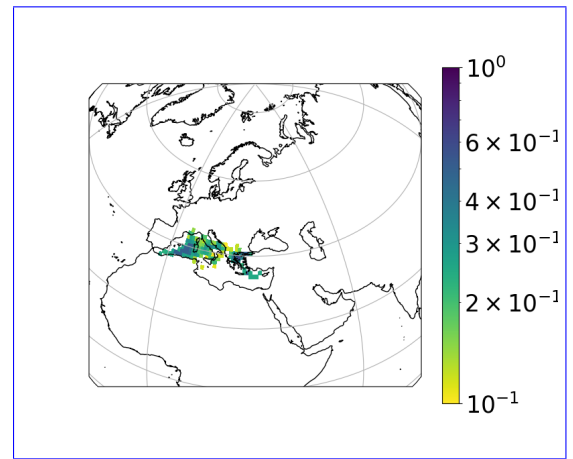
(b) Niksic
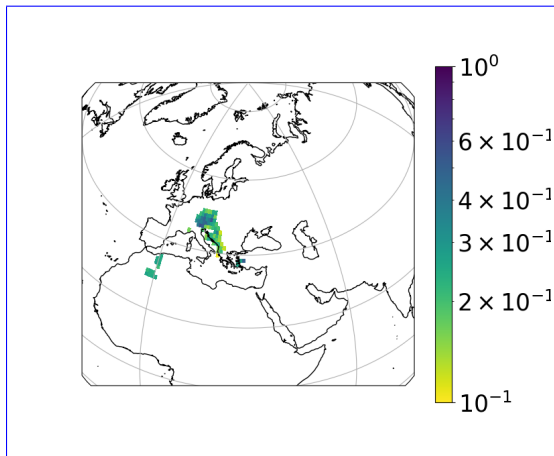
(c) Skopje
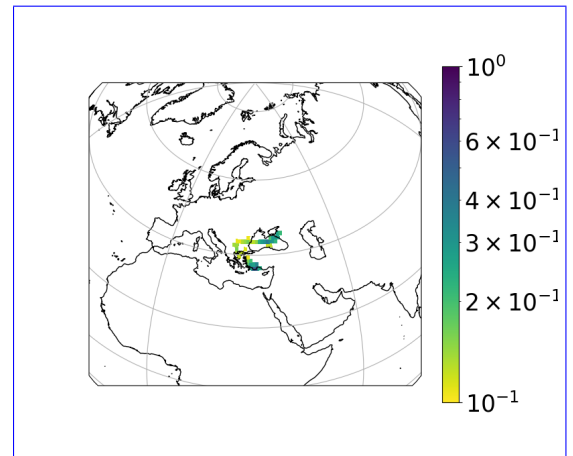
(d) Sofia
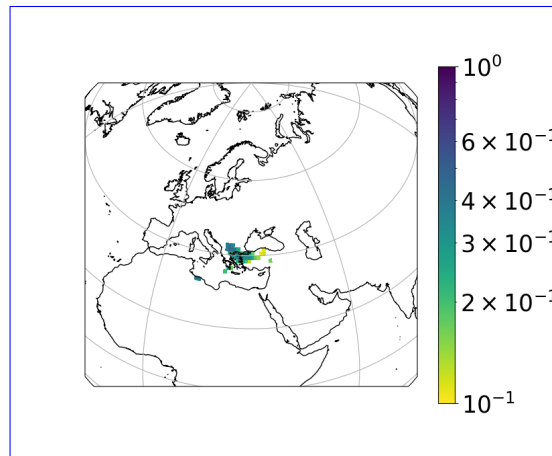
(e) Ankara

Figure A7. PSCF for ~~Dust~~ concentrations higher than the 90th per**27**ntile for dust aerosol ~~,~~ and for cities not included in Figure ~~7~~7. The vertical bar represents the PSCF ratio ($PSCF_{i,j} = weight_{i,j} * m_{i,j}/n_{i,j}$).
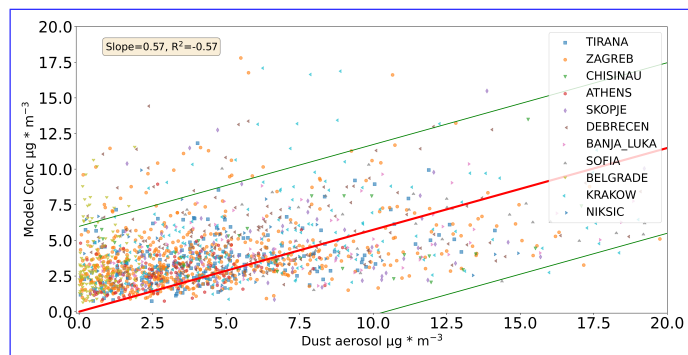
(a) secondary sulfate aerosol, solution for 14 cities, no intercept
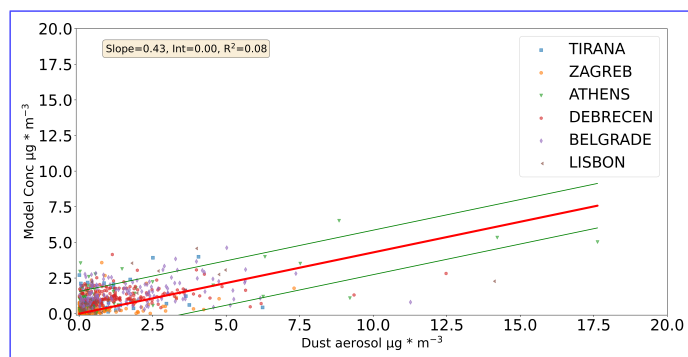
(b) dust aerosol solution, no intercept

Figure A8. Comparison between measured and modeled values based on Tikhonov regularization solutions, no intercept. ~~Regression~~ The solution for secondary sulfate using data from 14 cities is utilized in (a), while in (b) the dust aerosol emission fluxes for the Tikhonov regularization solution is used. The regression line $\pm$ 2 standard deviations is ~~depicted~~also presented. The measurement location is presented in the legend.

Disclaimer.

Acknowledgements. This research has been funded by the program "RER/1/015 - Apportioning air pollution sources on a regional scale", 2016 - 2017. We also acknowledge support of this work by the project "PANhellenic infrastructure for Atmospheric Composition and climatE change" (MIS 5021516), which is implemented under the Action "Reinforcement of the Research and Innovation Infrastructure", funded by the Operational Programme "Competitiveness, Entrepreneurship and Innovation" (NSRF 2014-2020) and co-financed by Greece and the European Union (European Regional Development Fund). We acknowledge support from the Zenodo repository for hosting the data files used in the manuscript.

460

References

Almeida, S., Manousakas, M., Diapouli, E., Kertesz, Z., Samek, L., Hristova, E., Šega, K., Alvarez, R. P., Belis, C., and Eleftheriadis, K.: Ambient particulate matter source apportionment using receptor modelling in European and Central Asia urban areas, Environmental Pollution, 266, 115 199, https://doi.org/10.1016/j.envpol.2020.115199, 2020.

Amato, F., Alastuey, A., Karanasiou, A., Lucarelli, F., Nava, S., Calzolai, G., Severi, M., Becagli, S., Gianelle, V. L., Colombi, C., Alves, C., Custódio, D., Nunes, T., Cerqueira, M., Pio, C., Eleftheriadis, K., Diapouli, E., Reche, C., Minguillón, M. C., Manousakas, M.-I., Maggos, T., Vratolis, S., Harrison, R. M., and Querol, X.: AIRUSE-LIFE+: a harmonized PM speciation and source apportionment in five southern European cities, Atmos. Chem. Phys., 16, 3289–3309, 2016.

Brown, S. G., Eberly, S., Paatero, P., and Norris, G. A.: Methods for estimating uncertainty in PMF solutions: Examples with ambient air and water quality data and guidance on reporting PMF results, Science of The Total Environment, 518–519, 626–635, https://doi.org/10.1016/j.scitotenv.2015.01.022, 2015.

Burkart, K., Causey, K., Cohen, A. J., Wozniak, S. S., Salvi, D. D., Abbafati, C., Adekanmbi, V., Adsuar, J. C., Ahmadi, K., Alahdab, F., Al-Aly, Z., Alipour, V., Alvis-Guzman, N., Amegah, A. K., Andrei, C. L., Andrei, T., Ansari, F., Arabloo, J., Aremu, O., Aripov, T., Babaee, E., Banach, M., Barnett, A., Bärnighausen, T. W., Bedi, N., Behzadifar, M., Béjot, Y., Bennett, D. A., Bensenor, I. M., Bernstein, R. S., Bhattacharyya, K., Bijani, A., Biondi, A., Bohlouli, S., Breitner, S., Brenner, H., Butt, Z. A., Cámera, L. A., Cantu-Brito, C., Carvalho, F., Cerin, E., Chattu, V. K., Chauhan, B. G., Choi, J.-Y. J., Chu, D.-T., Dai, X., Dandona, L., Dandona, R., Daryani, A., Davletov, K., de Courten, B., Demeke, F. M., Denova-Gutiérrez, E., Dharmaratne, S. D., Dhimal, M., Diaz, D., Djalalinia, S., Duncan, B. B., El Sayed Zaki, M., Eskandarieh, S., Fareed, M., Farzadfar, F., Fattahi, N., Fazlzadeh, M., Fernandes, E., Filip, I., Fischer, F., Foigt, N. A., Freitas, M., Ghashghaee, A., Gill, P. S., Ginawi, I. A., Gopalani, S. V., Guo, Y., Gupta, R. D., Habtewold, T. D., Hamadeh, R. R., Hamidi, S., Hankey, G. J., Hasanpoor, E., Hassen, H. Y., Hay, S. I., Heibati, B., Hole, M. K., Hossain, N., Househ, M., Irvani, S. S. N., Jaafari, J., Jakovljevic, M., Jha, R. P., Jonas, J. B., Jozwiak, J. J., Kasaeian, A., Kaydi, N., Khader, Y. S., Khafaie, M. A., Khan, E. A., Khan, J., Khan, M. N., Khatab, K., Khater, A. M., Kim, Y. J., Kimokoti, R. W., Kisa, A., Kivimäki, M., Knibbs, L. D., Kosen, S., Koul, P. A., Koyanagi, A., Kuate Defo, B., Kugbey, N., Lauriola, P., Lee, P. H., Leili, M., Lewycka, S., Li, S., Lim, L.-L., Linn, S., Liu, Y., Lorkowski, S., Mahasha, P. W., Mahotra, N. B., Majeed, A., Maleki, A., Malekzadeh, R., Mamun, A. A., Manafi, N., Martini, S., Meharie, B. G., Menezes, R. G., Mestrovic, T., Miazgowski, B., Miazgowski, T., Miller, T. R., Mini, G., Mirica, A., Mirrakhimov, E. M., Mohajer, B., Mohammed, S., Mohan, V., Mokdad, A. H., Monasta, L., Moraga, P., Morrison, S. D., Mueller, U. O., Mukhopadhyay, S., Mustafa, G., Muthupandian, S., Naik, G., Nangia, V., Ndwandwe, D. E., Negoi, R. I., Ningrum, D. N. A., Noubiap, J. J., Ogbo, F. A., Olagunju, A. T., Onwujekwe, O. E., Ortiz, A., Owolabi, M. O., P A, M., Panda-Jonas, S., Park, E.-K., Pashazadeh Kan, F., Pirsaheb, M., Postma, M. J., Pourjafar, H., Radfar, A., Rafiei, A., Rahim, F., Rahimi-Movaghar, V., Rahman, M. A., Rai, R. K., Ranabhat, C. L., Raoofi, S., Rawal, L., Renzaho, A. M. N., Rezapour, A., Ribeiro, D., Roever, L., Ronfani, L., Sabour, S., Saddik, B., Sadeghi, E., Saeedi Moghaddam, S., Sahebkar, A., Sahraian, M. A., Salimzadeh, H., Salvi, S. S., Samy, A. M., Sanabria, J., Sarmiento-Suárez, R., Sathish, T., Schmidt, M. I., Schutte, A. E., Sepanlou, S. G., Shaikh, M. A., Sharafi, K., Sheikh, A., Shigematsu, M., Shiri, R., Shirkoohi, R., Shuval, K., Soyiri, I. N., Tabarés-Seisdedos, R., Tefera, Y. M., Tehrani-Banihashemi, A., Temsah, M.-H., Thankappan, K. R., Topor-Madry, R., Tudor Car, L., Ullah, I., Vacante, M., Valdez, P. R., Vasankari, T. J., Violante, F. S., Waheed, Y., Wolfe, C. D. A., Yamada, T., Yonemoto, N., Yu, C., Zaman, S. B., Zhang, Y., Zodpey, S., Lim, S. S., Stanaway, J. D., and Brauer, M.: Estimates, trends, and drivers of the global burden of type 2 diabetes attributable to PM2·5 air pollution, 1990–2019: an analysis of data from the Global Burden of Disease Study 2019, The Lancet Planetary Health, 6, e586–e600, https://doi.org/10.1016/s2542-5196(22)00122-x, 2022.

Cavalli, F., Alastuey, A., Areskoug, H., Ceburnis, D., Čech, J., Genberg, J., Harrison, R., Jaffrezo, J., Kiss, G., Laj, P., Mihalopoulos, N., Perez, N., Quincey, P., Schwarz, J., Sellegri, K., Spindler, G., Swietlicki, E., Theodosi, C., Yttri, K., Aas, W., and Putaud, J.: A European aerosol phenomenology -4: Harmonized concentrations of carbonaceous aerosol at 10 regional background sites across Europe, Atmospheric Environment, 144, 133–145, https://doi.org/10.1016/j.atmosenv.2016.07.050, 2016.

Chen, P., Kang, S., Zhang, L., Abdullaev, S. F., Wan, X., Zheng, H., Maslov, V. A., Abdyzhapar uulu, S., Safarov, M. S., Tripathee, L., and Li, C.: Organic aerosol compositions and source estimation by molecular tracers in Dushanbe, Tajikistan, Environmental Pollution, 302, 119 055, https://doi.org/10.1016/j.envpol.2022.119055, 2022.

Diapouli, E., Manousakas, M. I., Vratolis, S., Vasilatou, V., Pateraki, S., Bairachtari, K. A., Querol, X., Amato, F., Alastuey, A., Karanasiou, A. A., Lucarelli, F., Nava, S., Calzolai, G., Gianelle, V. L., Colombi, C., Alves, C., Custódio, D., Pio, C., Spyrou, C., Kallos, G. B., and Eleftheriadis, K.: AIRUSE-LIFE + : estimation of natural source contributions to urban ambient air PM_{10} and $PM_{2.5}$ concentrations in southern Europe – implications to compliance with limit values, Atmos. Chem. Phys.,, 17, 3673–3685, 2017.

Donatelli, M. and Reichel, L.: Square smoothing regularization matrices with accurate boundary conditions, Journal of Computational and Applied Mathematics, 272, 334–349, https://doi.org/10.1016/j.cam.2013.08.015, 2014.

Eleftheriadis, K., Vratolis, S., and Nyeki, S.: Aerosol black carbon in the European Arctic: Measurements at Zeppelin station, Ny-Ålesund, Svalbard from 1998-2007, GEOPHYS RES LETT, 36, 2009.

EN12341: Determination of the PM10 fraction of suspended particulate matter - Reference method and field test procedure to demonstrate reference equivalence of measurement methods., Tech. rep., CEN, 1998.

Ghosh, R., Causey, K., Burkart, K., Wozniak, S., Cohen, A., and Brauer, M.: Ambient and household PM2.5 pollution and adverse perinatal outcomes: A meta-regression and analysis of attributable global burden for 204 countries and territories, PLOS Medicine, 18, e1003 718, https://doi.org/10.1371/journal.pmed.1003718, 2021.

Gini, M., Manousakas, M., Karydas, A., and Eleftheriadis, K.: Mass size distributions, composition and dose estimates of particulate matter in Saharan dust outbreaks, Environmental Pollution, 298, 118 768, https://doi.org/10.1016/j.envpol.2021.118768, 2022.

Hansen, P. C.: Analysis of Discrete Ill-Posed Problems by Means of the L-Curve, SIAM Review, 34, 561–580, https://doi.org/10.1137/1034115, 1992.

IDAEA: AIRUSE: Testing and development of air quality mitigation measures in Southern Europe, LIFE11/ENV/ES/584, 2016.

Johnson, T., Guttikunda, S., Wells, G., Artaxo, P., Bond, T., Russell, A., Watson, J., and West, J.: Tools for Improving Air Quality Management: A Review of Top-Down Source Apportionment Techniques and Their Application in Developing Countries, World Bank, Washington, DC, 2011.

Klimont, Z., Kupiainen, K., Heyes, C., Purohit, P., Cofala, J., Rafaj, P., Borken-Kleefeld, J., and Schöpp, W.: Global anthropogenic emissions of particulate matter including black carbon, Atmospheric Chemistry and Physics, 17, 8681–8723, https://doi.org/10.5194/acp-17-8681-2017, 2017.

Laden, F., Schwartz, J., Speizer, F. E., and Dockery, D. W.: Reduction in Fine Particulate Air Pollution and Mortality: Extended Follow-up of the Harvard Six Cities Study, Am. J. Respir. Crit. Care Med., 173, 667–672, https://doi.org/10.1164/rccm.200503-443OC, 2006.

Liu, F., Choi, S., Li, C., Fioletov, V. E., McLinden, C. A., Joiner, J., Krotkov, N. A., Bian, H., Janssens-Maenhout, G., Darmenov, A. S., and da Silva, A. M.: A new global anthropogenic SO2 emission inventory for the last decade: a mosaic of satellite-derived and bottom-up emissions, Atmospheric Chemistry and Physics, 18, 16 571–16 586, https://doi.org/10.5194/acp-18-16571-2018, 2018.

Lohmann, U. and Feichter, J.: Global indirect aerosol effects: a review, Atmos. Chem. Phys., 5, 715–737, https://doi.org/10.5194/acp-5-715-2005, 2005.

Manousakas, M., Diapouli, E., Papaefthymiou, H., Kantarelou, V., Zarkadas, C., Kalogridis, A.-C., A.-G., K., and Eleftheriadis, K.: XRF characterization and source apportionment of PM10 samples collected in a coastal city, X-Ray Spectrometry, p. 1–11, https://doi.org/10.1002/xrs.2817, 2017a.

Manousakas, M., Papaefthymiou, H., Diapouli, E., Migliori, A., Karydas, A. G., Bogdanovic-Radovic, I., and Eleftheriadis, K.: Assessment of PM2.5 sources and their corresponding level of uncertainty in a coastal urban area using EPA PMF 5.0 enhanced diagnostics., Sci Total Environ, 574, 155–164, https://doi.org/10.1016/j.scitotenv.2016.09.047, 2017b.

Mantas, E., Remoundaki, E., Halari, I., Kassomenos, P., Theodosi, C., Hatzikioseyian, A., and Mihalopoulos, N.: Mass closure and source apportionment of PM$_{2.5}$ by Positive Matrix Factorization analysis in urban Mediterranean environment, Atmos. Environ., 94, 154–163, 2014.

Pandey, A., Brauer, M., Cropper, M. L., Balakrishnan, K., Mathur, P., Dey, S., Turkgulu, B., Kumar, G. A., Khare, M., Beig, G., Gupta, T., Krishnankutty, R. P., Causey, K., Cohen, A. J., Bhargava, S., Aggarwal, A. N., Agrawal, A., Awasthi, S., Bennitt, F., Bhagwat, S., Bhanumati, P., Burkart, K., Chakma, J. K., Chiles, T. C., Chowdhury, S., Christopher, D. J., Dey, S., Fisher, S., Fraumeni, B., Fuller, R., Ghoshal, A. G., Golechha, M. J., Gupta, P. C., Gupta, R., Gupta, R., Gupta, S., Guttikunda, S., Hanrahan, D., Harikrishnan, S., Jeemon, P., Joshi, T. K., Kant, R., Kant, S., Kaur, T., Koul, P. A., Kumar, P., Kumar, R., Larson, S. L., Lodha, R., Madhipatla, K. K., Mahesh, P. A., Malhotra, R., Managi, S., Martin, K., Mathai, M., Mathew, J. L., Mehrotra, R., Mohan, B. V. M., Mohan, V., Mukhopadhyay, S., Mutreja, P., Naik, N., Nair, S., Pandian, J. D., Pant, P., Perianayagam, A., Prabhakaran, D., Prabhakaran, P., Rath, G. K., Ravi, S., Roy, A., Sabde, Y. D., Salvi, S., Sambandam, S., Sharma, B., Sharma, M., Sharma, S., Sharma, R. S., Shrivastava, A., Singh, S., Singh, V., Smith, R., Stanaway, J. D., Taghian, G., Tandon, N., Thakur, J. S., Thomas, N. J., Toteja, G. S., Varghese, C. M., Venkataraman, C., Venugopal, K. N., Walker, K. D., Watson, A. Y., Wozniak, S., Xavier, D., Yadama, G. N., Yadav, G., Shukla, D. K., Bekedam, H. J., Reddy, K. S., Guleria, R., Vos, T., Lim, S. S., Dandona, R., Kumar, S., Kumar, P., Landrigan, P. J., and Dandona, L.: Health and economic impact of air pollution in the states of India: the Global Burden of Disease Study 2019, The Lancet Planetary Health, 5, e25–e38, https://doi.org/10.1016/s2542-5196(20)30298-9, 2021.

Panteliadis, P., Hafkenscheid, T., Cary, B., Diapouli, E., Fischer, A., Favez, O., Quincey, P., Viana, M., Hitzenberger, R., Vecchi, R., Saraga, D., Sciare, J., Jaffrezo, J. L., John, A., Schwarz, J., Giannoni, M., Novak, J., Karanasiou, A., Fermo, P., and Maenhaut, W.: ECOC comparison exercise with identical thermal protocols after temperature offsets correction – instrument diagnostics by in-depth evaluation of operational parameters., Atmos. Meas. Tech., 8(2), 779–792, 2015.

Park, Y., Reichel, L., Rodriguez, G., and Yu, X.: Parameter determination for Tikhonov regularization problems in general form, Journal of Computational and Applied Mathematics, 343, 12–25, https://doi.org/10.1016/j.cam.2018.04.049, 2018.

Perrone, M. G., Vratolis, S., Georgieva, E., Torok, S., Sega, K., Veleva, B., Osan, J., Beslic, I., Kertesz, Z., Pernigotti, D., Eleftheriadis, K., and Bellis, C. A.: Sources and geographic origin of particulate matter in urban areas of the Danube macro-region: the cases of Zagreb (Croatia), Budapest (Hungary) and Sofia (Bulgaria), Sci. Total Environ., 619-620, 1515–1529, 2018.

Pisso, I., Sollum, E., Grythe, H., Kristiansen, N. I., Cassiani, M., Eckhardt, S., Arnold, D., Morton, D., Thompson, R. L., Groot Zwaaftink, C. D., Evangeliou, N., Sodemann, H., Haimberger, L., Henne, S., Brunner, D., Burkhart, J. F., Fouilloux, A., Brioude, J., Philipp, A., Seibert, P., and Stohl, A.: The Lagrangian particle dispersion model FLEXPART version 10.4, Geoscientific Model Development, 12, 4955–4997, https://doi.org/10.5194/gmd-12-4955-2019, 2019.

Polissar, A. V., Hopke, P. K., and Harris, J. M.: Source Regions for Atmospheric Aerosol Measured at Barrow, Alaska, Environmental Science & Technology, 35, 4214–4226, https://doi.org/10.1021/es0107529, 2001.

575 Pope, C. A. I. and Dockery, D. W.: Health Effects of Fine Particulate Air Pollution: Lines that Connect, JAPCA J. Air Waste Ma., 56, 709–742, 2006.

Rodhe, H.: Budgets and turn-over times of atmospheric sulfur compounds, Atmospheric Environment (1967), 12, 671–680, https://doi.org/10.1016/0004-6981(78)90247-0, 1978.

Seinfeld, J. H. and Pandis, S. N.: Atmospheric Chemistry and Physics: From Air Pollution to Climate Change, Wiley Interscience, 1998.

580 Stohl, A., Forster, C., Frank, A., Seibert, P., and Wotawa, G.: Technical Note: The Lagrangian particle dispersion model FLEXPART version 6.2, Atmos. Chem. Phys, 5, 2461–2474, 2005.

Stohl, A., Seibert, P., Arduini, J., Eckhardt, S., Fraser, P., Greally, B. R., Lunder, C., Maione, M., Mühle, J., O'Doherty, S., Prinn, R. G., Reimann, S., Saito, T., Schmidbauer, N., Simmonds, P. G., Vollmer, M. K., Weiss, R. F., and Yokouchi, Y.: An analytical inversion method for determining regional and global emissions of greenhouse gases: Sensitivity studies and application to halocarbons, Atmospheric

585 Chemistry and Physics, 9, 1597–1620, https://doi.org/10.5194/acp-9-1597-2009, 2009.

Tikhonov, A. N., Goncharsky, A. V., Stepanov, V. V., and Yagola, A. G.: Numerical Methods for the Solution of Ill-Posed Problems, https://doi.org/10.1007/978-94-015-8480-7, 1995.

Valentine, A. P. and Sambridge, M.: Optimal regularization for a class of linear inverse problem, Geophysical Journal International, 215, 1003–1021, https://doi.org/10.1093/gji/ggy303, 2018.

590 Viana, M., Chi, X., Maenhaut, W., Cafmeyer, J., Querol, X., Alastuey, A., Mikuška, P., and Večeřa, Z.: Influence of Sampling Artefacts on Measured PM, OC, and EC Levels in Carbonaceous Aerosols in an Urban Area, Aerosol Science and Technology, 40, 107–117, https://doi.org/10.1080/02786820500484388, 2006.

Vratolis, S., Fetfatzis, P., Argyrouli, A., Papayannis, A., Muller, D., Veselovskii, I., Bougiatioti, A., Nenes, A., Remoundaki, E., Diapouli, E., Manousakas, M., Mylonaki, M., and Eleftheriadis, K.: A new method to retrieve the real part of the equivalent refractive index of

595 atmospheric aerosols, Journal of Aerosol Science, 117, 54–62, 2018.

Wesseling, J., Pisoni, E., Guevara, M., Janssen, S., Tarrason, L., Clappier, A., Thunis, P., Guerreiro, C., Pirovano, G., González Ortiz, A., Monteiro, A., and Belis, C.: Recommendations regarding modelling applications within the scope of the ambient air quality directives, European Commission Joint Research Centre, https://doi.org/10.2760/819240, 2019.

WHO: WHO global air quality guidelines. Particulate matter (PM 2.5 and PM 10), ozone, nitrogen dioxide, sulfur dioxide and carbon

600 monoxide, Tech. rep., World Health Organization, 2021.